

INTERNSHIP REPORT

# Simulations of sympathetic cooling of an anion with a cation

**ETH** zürich

ESPCI  PARIS | PSL 

Andreas Fyrillas

*Project supervisor:* Daniel Kienzler

Trapped ion Quantum Information Group

*Host university:* ETH Zurich, Otto-Stern-Weg 1, HPF E10,8093 Zürich, Schweiz

*Student university:* Ecole Supérieure de Physique et de Chimie de la ville de Paris, 10 rue Vauquelin, 75005 Paris

May-August 2020

# Acknowledgements

I would like to thank Daniel Kienzler for giving me the opportunity to work with the TIQI group, for proposing a subject I could work on from Paris and for making sure we could meet every day to discuss my results. I thank Jonathan Home, Matthew Grau and Chi Zhang for their insightful questions and comments during the group meetings.

Special thanks to my cat Achille as well.

# Abstract

The use of different ions species in the context of quantum technologies could offer new possibilities and advantages in contrast to same-ion systems. The trapped ions need to be cooled beforehand in order to manipulate them as quantum systems. We investigate the sympathetic cooling of a trapped hot  $D^-$  by a trapped  $Be^+$  held cold by laser cooling. We study if the sympathetic cooling is possible and which parameters are the most relevant during this process, by simulating the trajectories of the ions using classical equations of motion and a semi-classical approach for the radiation pressure and photon scattering. We show that there are restrictions on the trap geometries when manipulating ions of opposite charges and that sympathetically cooling  $D^-$  by  $Be^+$  is possible when the radial trap frequency is sufficiently low. We find that the cooling rate is higher if the ions are brought closer to each other in the ion trap, or if the laser power is more intense, up to a certain limit. The outreach of the mentioned results is not limited to the  $(D^- + Be^+)$  and should apply as well to the sympathetic cooling of other ion species.

# Contents

<b>1</b>	<b>Introduction</b>	<b>1</b>
<b>2</b>	<b>Trapped ions</b>	<b>3</b>
2.1	Introduction to ion trapping . . . . .	3
2.1.1	A few lines about classical electrodynamics . . . . .	3
2.1.2	Trapping an ion . . . . .	5
2.1.3	Pseudopotentials . . . . .	7
2.1.4	Coupling trapped cations . . . . .	9
2.2	Sympathetic cooling of $D^-$ with $Be^+$ . . . . .	10
2.2.1	Coupling a trapped cation with an anion . . . . .	10
2.2.2	Sympathetic cooling of the system . . . . .	11
<b>3</b>	<b>Simulation code</b>	<b>13</b>
3.1	Modification of CPsim . . . . .	13
3.2	Physical model . . . . .	14
3.2.1	System . . . . .	14
3.2.2	Interaction with the laser beam . . . . .	16
3.2.3	Equation of motion . . . . .	18
3.3	Total energy . . . . .	19
3.3.1	Kinetic energy . . . . .	19
3.3.2	$Be^+$ potential energy . . . . .	20
3.3.3	$D^-$ potential energy . . . . .	20
3.3.4	interaction energy . . . . .	20
3.3.5	Rest energy . . . . .	20
<b>4</b>	<b>Results</b>	<b>21</b>
4.1	Trap stability . . . . .	21
4.2	$Be^+$ laser cooling . . . . .	22
4.2.1	Trap frequency . . . . .	23
4.2.2	Laser detuning . . . . .	23
4.2.3	Laser power . . . . .	24
4.3	Sympathetic cooling . . . . .	25
4.3.1	Radial trap frequency . . . . .	25
4.3.2	Distance between wells . . . . .	26
4.3.3	Laser saturation parameter . . . . .	26

4.3.4	Laser detuning and orientation . . . . .	27
4.3.5	Steady state . . . . .	28
4.3.6	Comparison with a more realistic electric field . . . . .	29
4.3.7	Trap modulation . . . . .	31
<b>5</b>	<b>Discussion and Conclusion</b>	<b>33</b>
	<b>Appendices</b>	<b>35</b>
<b>A</b>	<b>Coupled harmonic oscillators in the cubic trap</b>	<b>36</b>
A.1	Presentation of the system . . . . .	36
A.2	Lagrangian of the system . . . . .	37
A.3	Rest position . . . . .	37
A.4	Taylor expansion of the Lagrangian . . . . .	39
A.4.1	Electric potential energy . . . . .	39
A.4.2	Interaction energy . . . . .	40
A.4.3	Lagrangian . . . . .	40
A.5	Hamiltonian . . . . .	40
A.6	Equations of motion . . . . .	41
A.7	Initial conditions . . . . .	42
A.8	Beating . . . . .	43
A.9	Damping . . . . .	44
<b>B</b>	<b>Laser manipulation of atoms</b>	<b>45</b>
B.1	Light intensity . . . . .	45
B.2	Atomic saturation parameter . . . . .	46
B.3	Radiation pressure . . . . .	46
B.4	Dipole force . . . . .	47
<b>C</b>	<b>Piecewise quadratic interpolation of the electric potential</b>	<b>48</b>

# Chapter 1

## Introduction

In the 1950s, Wolfgang Paul and Hans Dehmelt invented the Paul trap and the Penning trap, devices capable of trapping charged particles and they were awarded the Nobel prize in 1989 for their work. This device laid the foundation for a set of advanced quantum technologies, like quantum logic spectroscopy [1]. With the rising interest in quantum computing, it was also shown that is possible to construct quantum computers with trapped ions [2]. Each ion would represent a qubit, and quantum gate operations would be performed using lasers interacting with the ions. Today, many trapped ions experiments use miniaturized ion trap arrays (Fig.1.1). This has the advantage of greatly reducing the size of the devices used for trapping ions, while paving the way for quantum computing chips.

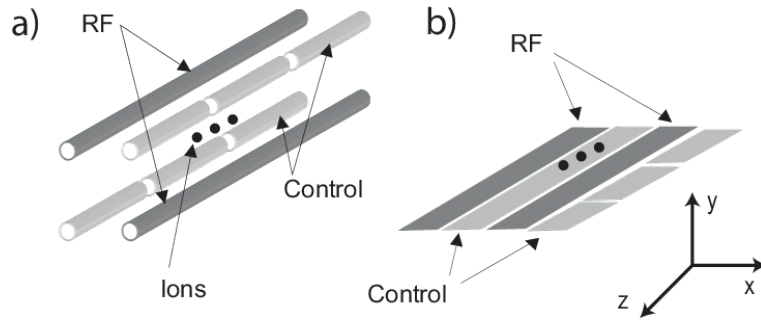


**Figure 1.1:** (a) Standard linear RF Paul trap; (b) Surface electrode geometry where all electrodes reside in a single plane, with the ions trapped above this plane. Picture taken from [3].

The different ions interact with each other through the Coulomb force, and usually only cations are used. Interactions between ions consisting of cations and anions have not yet been experimentally tested, but could potentially offer advantages over same-species systems. Upcoming experiments will start to use cation-anion quantum logic spectroscopy. For instance, the BASE collaboration (Baryon Antibaryon Symmetry Experiment) will study the fundamental symmetries of the Standard Model by coupling a trapped antiproton (which is charged negatively) with a trapped Beryllium+ ( $\text{Be}^+$ ) ion [4].

At ETH Zurich, the Trapped Ion Quantum Information Group is designing an experiment to investigate the possibilities offered by trapped ions of opposite charges, which is the context of this internship.

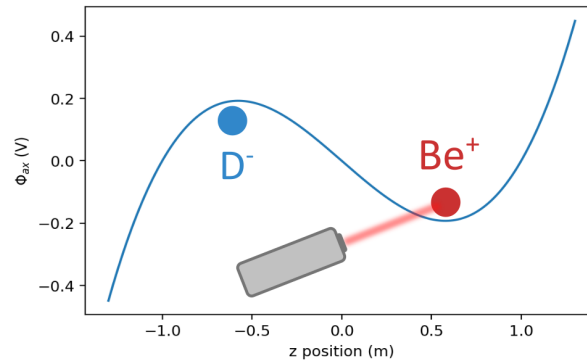


**Figure 1.2:** *Drawing of the experiment*

The internship focuses on one particular aspect of the experiment, which will use a  $Be^+$  cation and a Deuterium- ( $D^-$ ) anion (Fig.1.2). The  $D^-$  ions was chosen because it is the mass-charge equivalent of anti- $H_2^+$ , which would be interesting to study for looking into matter-antimatter asymmetry. In order to be able to perform operations on the ions, it is necessary that they are cooled beforehand in the ion trap. It is easily possible to laser cool the  $Be^+$  because it possesses a closed cycling transition. On the contrary,  $D^-$  has to be cooled indirectly: it is cooled sympathetically through the Coulomb interaction between the ions. Concretely, the external degrees of freedom of  $Be^+$  and  $D^-$  are coupled by the Coulomb force the ions exert on each other, thus the ions exchange energy between each other. The energy transferred from  $D^-$  to  $Be^+$  is efficiently removed from the system because of the laser cooling.

The objective of this internship is to study the parameters affecting the cooling, as well as to provide an order of magnitude for the time needed to sympathetically cool the system.

# Chapter 2

## Trapped ions

### 2.1 Introduction to ion trapping

#### 2.1.1 A few lines about classical electrodynamics

The electric field  $\mathbf{E}$ <sup>1</sup> and magnetic field  $\mathbf{B}$  are vector fields defined in a given region of space. We consider that the sources creating the fields are outside the region of interest. The fields obey then the following set of Maxwell equations:

$$\begin{aligned}\nabla \mathbf{E} &= 0 \\ \nabla \mathbf{B} &= 0 \\ \nabla \wedge \mathbf{E} &= -\frac{\partial \mathbf{B}}{\partial t} \\ \nabla \wedge \mathbf{B} &= \frac{1}{c^2} \frac{\partial \mathbf{E}}{\partial t}\end{aligned}$$

with  $c \approx 3 \times 10^8$  m/s the speed of light in vacuum. The magnetic field created by the electric field is negligible if the following condition is met:

$$\frac{\|\mathbf{B}\|}{\|\mathbf{E}\|} \approx \frac{\frac{\|\mathbf{E}\|L}{c^2\tau}}{\|\mathbf{E}\|} = \frac{L}{c^2\tau} \ll 1$$

where  $L$  is a typical length of the system and  $\tau$  a typical time scale. We have used the fourth Maxwell equation to get an order of magnitude for  $\|\mathbf{B}\|$ .

Typically, we will work with  $L = 20\mu\text{m}$  and  $\tau = \frac{1}{50\text{MHz}} = 20\text{ns}$ , which largely satisfy the stated condition. Therefore, we will simply neglect the magnetic field.

We will often make use of the scalar electric potential from which the electric field can be derived using the following formula (only valid in our approximation, otherwise we would have to add the magnetic vector potential):

---

<sup>1</sup>Vectors are written in bold

$$\mathbf{E} = -\nabla\Phi$$

The electric potential in the absence of sources obeys the Laplace equation, a direct consequence of Maxwell's equations:

$$\nabla^2\Phi = 0$$

A particle which carries a charge  $q$  in the presence of an electric field will feel the electric Lorentz force:

$$\mathbf{F}_{el} = q\mathbf{E} = -q\nabla\Phi$$

meaning, the particle will be attracted by potential wells if it is charged positively, and by potential peaks if it is charged negatively.

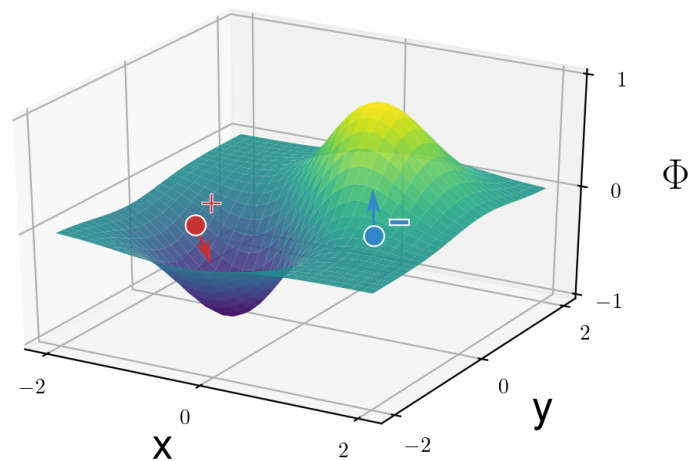


**Figure 2.1:** Red particle with a positive charge attracted by a potential well, blue particle with negative charge attracted by a potential peak.

In fact, we can even define a potential energy associated with the electric potential:

$$\mathcal{E}_{pot} = q\Phi$$

Last but not least, the electric field created by a static point charge  $q$  located in  $\mathbf{x}_0$  is given by Coulomb's law:

$$\mathbf{E}(\mathbf{x}) = \frac{q}{4\pi\epsilon_0} \frac{\mathbf{x} - \mathbf{x}_0}{\|\mathbf{x} - \mathbf{x}_0\|^3}$$

whose associated electric potential is:

$$\Phi_{Coul} = \frac{q}{4\pi\epsilon_0} \frac{1}{\|\mathbf{x} - \mathbf{x}_0\|}$$

These are classical results from electrodynamics, and can be easily found in any textbook on the matter [5, 6].

### 2.1.2 Trapping an ion

Ions carry an electric charge and can therefore be moved by electric fields. One might think that trapping an ion in a static potential should be very easy using a confining electric field in all 3 directions of space, like in Fig.2.2. While it is physically possible to produce a confining electric field in 2 dimensions, it will generally be anti-confining in the third dimension, because in the end it has to obey Maxwell's equations. The impossibility of confining an ion in 3D with a static electric field is a consequence of Earnshaw's theorem from electrostatics.

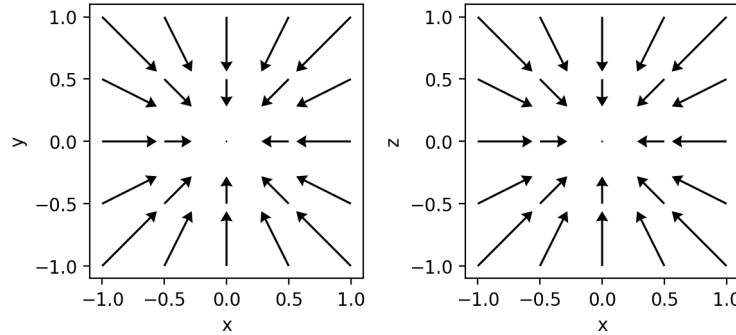


**Figure 2.2:** Unrealistic electric field confining in all 3 directions of space.

Thus, trapping an ion takes a more sophisticated device. The ion trap we will describe is called a linear Paul trap. It is a superposition of two electric fields created by the following potentials [7]:

$$\Phi_{ax}(x, y, z) = \frac{1}{2} U_{ax} (\alpha_{ax} x^2 + \beta_{ax} y^2 + \gamma_{ax} z^2)$$

$$\Phi_{rad}(x, y, z, t) = \frac{1}{2} U_{rad} \cos(\omega_{rf} t) \alpha_{rad} (x^2 - y^2)$$

$U$  represents the potential's amplitude.  $\Phi_{ax}$  is responsible for trapping the ion in the axial direction ( $z$  axis), while  $\Phi_{rad}$  takes care of the radial directions ( $x$  and  $y$  axis). The radial trap oscillation

frequency  $f_{rf} = \frac{\omega_{rf}}{2\pi}$  is typically in the MHz range. The Laplace equation imposes the following condition:

$$-\alpha_{ax} - \beta_{ax} = \gamma_{ax} > 0$$

Note that  $\Phi_{ax}$  has to be anti-confining in the  $x$  or  $y$  axis in order to be confining in the axial  $z$  direction, so there is a competition between  $\Phi_{ax}$  pushing the ion out of the trap radially and  $\Phi_{rad}$  keeping the ion confined. In practice, this translates into having to apply high voltages on the radial trap..

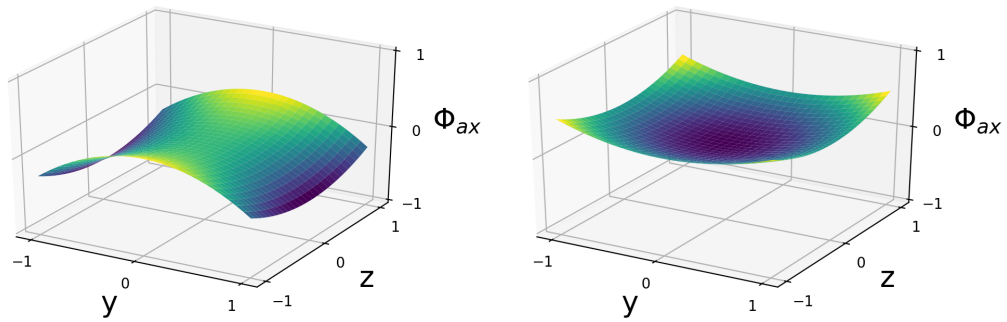


**Figure 2.3:** Plot of  $\Phi_{ax}$  in Volts as a function of  $x, y$  and  $z$  for  $U_{ax} = 1V$ ,  $\alpha_{rad} = -1m^{-2}$ ,  $\beta_{rad} = 0.5m^{-2}$  and  $\gamma_{rad} = 0.5m^{-2}$ . Axial potential is anti-confining in the  $x$  direction and confining in the other two (for a cation).

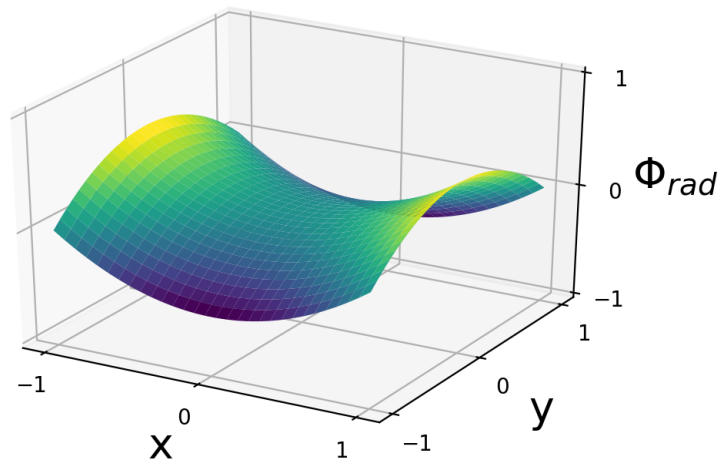


**Figure 2.4:** Plot of  $\Phi_{rad}$  in Volts as a function of  $x$  and  $y$  for  $t = 0$ ,  $U_{rad} = 1V$  and  $\alpha_{rad} = 1m^{-2}$ .

Also, it is important to keep in mind that in real life it is not possible to create such perfect harmonic potentials, because higher order terms appear in real traps. The expression of the radial and axial potentials is for that reason to be considered as an approximation of their shape at the center of the trap.

### 2.1.3 Pseudopotentials

#### Mathieu's differential equation

If we put an ion with charge  $q$  in the linear Paul trap, it will obey the following equations of motion in the context of classical mechanics:

$$\begin{aligned}\ddot{x}(t) &= -q \frac{\partial(\Phi_{ax} + \Phi_{rad})}{\partial x} = -qU_{ax}\alpha_{ax}x - qU_{rad}\alpha_{rad}\cos(\omega_{rf}t)x \\ \ddot{y}(t) &= -q \frac{\partial(\Phi_{ax} + \Phi_{rad})}{\partial y} = -qU_{ax}\beta_{ax}y + qU_{rad}\alpha_{rad}\cos(\omega_{rf}t)y \\ \ddot{z}(t) &= -q \frac{\partial(\Phi_{ax} + \Phi_{rad})}{\partial z} = -qU_{ax}\gamma_{ax}z\end{aligned}$$

These differential equations aren't coupled and the solution for the  $z$  position is a simple harmonic motion. We focus on the solution of the  $x$  position, as the  $y$  position is treated in a similar fashion.

The equation on the  $x$  position is far from a simple harmonic oscillator differential equation and difficult to solve. Fortunately, French mathematician Émile Léonard Mathieu (1835-1890) paved the way for us by showing that it is possible to write an analytic (but still complicated) solution for this equation, which is of the form of Mathieu's differential equation:

$$\frac{d^2x}{d\tau^2} + (a_x - 2b_x \cos(2\tau))x = 0$$

with

$$\begin{aligned}a_x &= \frac{4qU_{ax}\alpha_{ax}}{m\omega_{rf}^2} \\ b_x &= -\frac{2qU_{rad}\alpha_{rad}}{m\omega_{rf}^2} \\ \tau &= \frac{\omega_{rf}}{2}t\end{aligned}$$

#### Solution at lowest order

At lowest order, if  $|a_x|, b_x^2 \ll 1$  and if the particle starts at position  $x = 0$  with some initial velocity, the solution for the  $x$  position of the particle can be written as [7]:

$$x(t) = 2A \cos\left(\frac{\beta_x \omega_{rf}}{2}t\right) \left(1 - \frac{b_x}{2} \cos(\omega_{rf}t)\right)$$

with

$$\beta_x = \sqrt{a_x + \frac{b_x^2}{2}}$$

It is a superposition of harmonic oscillations at pulsation  $\frac{\beta_x \omega_{rf}}{2}$  called the secular motion and fast oscillations at pulsation  $\omega_{rf}$  dubbed micromotion.

### Pseudopotential

We can get the lowest order solution also by replacing the time dependent radial potential by a constant "pseudopotential" , whose expression is [8]:

$$\Phi_{rad,ps} = \frac{q}{4m\omega_{rf}^2} (\nabla \Phi_{rad}^0)^2$$

with  $\Phi_{rad}^0$  the shape of the potential  $\Phi_{rad}$  without oscillations:

$$\begin{aligned}\Phi_{rad} &= \Phi_{rad}^0 \cos(\omega_{rf} t) \\ \Phi_{rad}^0 &= \frac{1}{2} U_{rad} \alpha_{rad} (x^2 - y^2)\end{aligned}$$

If we solve this simpler equation instead:

$$\ddot{x}(t) = -q \frac{\partial(\Phi_{ax} + \Phi_{rad,ps})}{\partial x}$$

then we get a reasonable approximation of the analytic solution of Mathieu's differential equation.

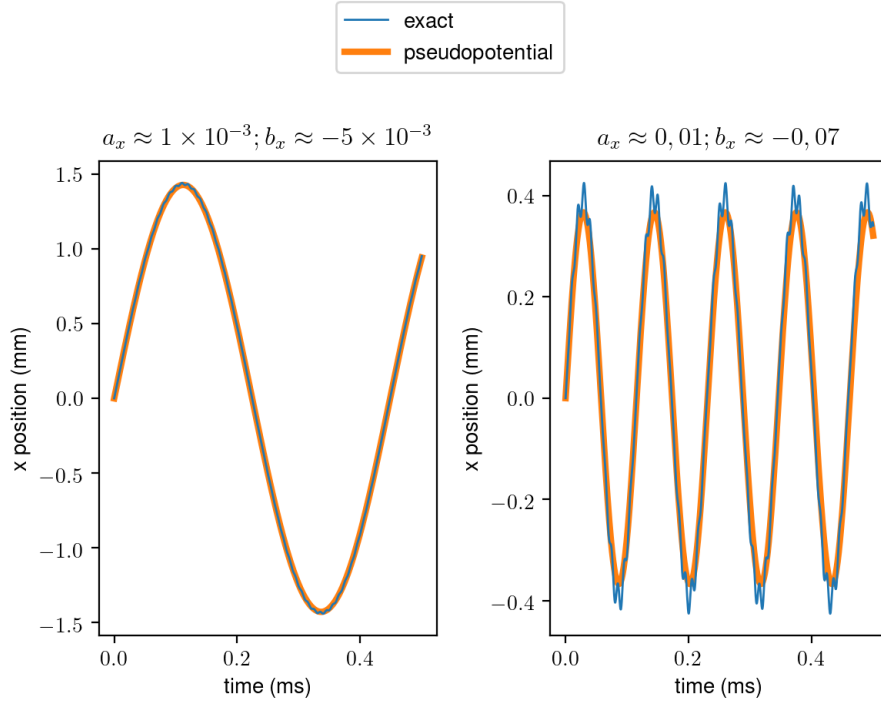


**Figure 2.5:** Plot of  $x$  as a function of time for a proton with  $\omega_{rad} = 100$  kHz. Left: small parameters, the pseudopotential solution replicates with good fidelity the exact solution. Right: larger parameters, pseudopotential method hits its limits.

### 2.1.4 Coupling trapped cations

It is possible to trap two cations separately in their own potential well, while enabling them to interact via the Coulomb interaction. Such a system can be used to study coupled quantized mechanical oscillators [9, 10]. For that purpose, the axial potential must be of the form:

$$\Phi_{ax}(x, y, z) = \frac{1}{2} U_{ax} (\alpha_{ax} z^4 + \beta_{ax} z^2) + f(x, y)$$

with  $f(x, y)$  a function chosen in order that  $\Phi_{ax}$  satisfies the Laplace equation. We can keep however the same quadratic radial potential as before:

$$\Phi_{rad}(x, y, z, t) = \frac{1}{2} U_{rad} \cos(\omega_{rf} t) \alpha_{rad} (x^2 - y^2)$$

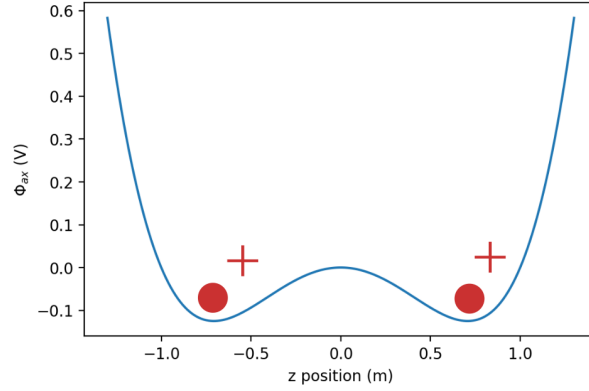


**Figure 2.6:** Plot of  $\Phi_{ax}$  as a function of  $z$ . Two cations can be trapped in separate wells using this trap geometry. Parameters:  $\alpha_{ax} = 1 \text{ m}^{-4}$ ;  $\beta_{ax} = -1 \text{ m}^{-2}$ ;  $U_{ax} = 1 \text{ V}$

## 2.2 Sympathetic cooling of $\text{D}^-$ with $\text{Be}^+$

### 2.2.1 Coupling a trapped cation with an anion

In principle, we can adapt the cation-cation coupling method to a cation-anion system. In our case, we want to couple  $\text{Be}^+$  with  $\text{D}^-$ . We will therefore use a cubic axial potential of the form:

$$\Phi_{ax}(x, y, z) = \frac{1}{2}U_{ax}(\alpha_{ax}z^3 + \beta_{ax}z) + f(x, y)$$

with  $f(x, y)$  a function chosen in order that  $\Phi_{ax}$  satisfies the Laplace equation. This type of cubic trap potential requires lower voltages in principle than the quartic potential using the same electrodes (see Suchita Agrawal's report). We keep the quadratic radial trap for radial confinement, as in the previous sections.

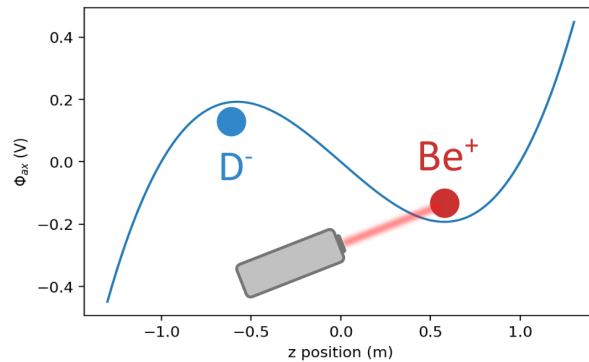


**Figure 2.7:** Plot of  $\Phi_{ax}$  as a function of  $z$ .  $\text{Be}^+$  and  $\text{D}^-$  can be trapped in separate wells using this trap geometry.  $\text{Be}^+$  is laser cooled. Parameters:  $\alpha_{ax} = 1 \text{ m}^{-3}$ ;  $\beta_{ax} = -1 \text{ m}^{-1}$ ;  $U_{ax} = 1 \text{ V}$  Note that these do not represent the values with intent to use experimentally.

## 2.2.2 Sympathetic cooling of the system

### Definition

In general, sympathetic cooling is the act of using one particle species to cool a second one. For instance, one could think of cooling a gas of hot atoms by mixing it with a gas of cold atoms. The object of this project is also considered as sympathetic cooling: we use a laser-cooled  $\text{Be}^+$  to cool a hot  $\text{D}^-$  via the Coulomb interaction (Fig. 2.7).

The objective is to transfer as fast as possible  $\text{D}^-$ 's kinetic energy to  $\text{Be}^+$ , because  $\text{Be}^+$ 's motion is damped by laser cooling.

### Coupled harmonic oscillators

To get a sense of how we expect the system to behave, we will start with a very simple case and work our way through to a more complex, but realistic, situation.

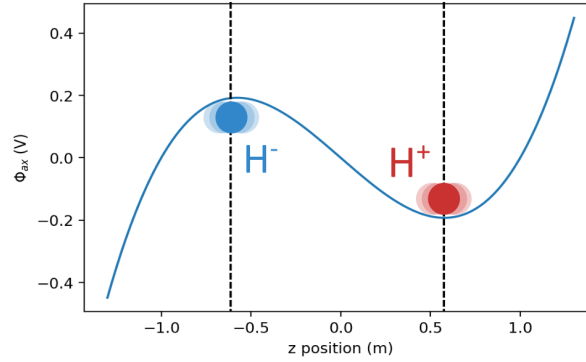


**Figure 2.8:** Small oscillations of  $\text{H}^-$  and  $\text{H}^+$  around their rest position. Dashed lines represent the local extrema of the axial trap along the  $z$  direction.

We start with two ions of the same mass:  $\text{H}^-$  and  $\text{H}^+$ . Let us consider that the ions don't interact with each other and only move on the  $z$  axis in their respective well (this way they only feel the cubic axial potential). We consider small oscillations. In this approximation, each ion represents a harmonic oscillator which vibrates with a frequency

$$f = \frac{1}{2\pi} \sqrt{\frac{q}{m} \frac{\partial^2 \Phi_{ax}}{\partial z^2}}$$

along the  $z$  axis. The ions oscillate at the same frequency because the trap is symmetric with respect to the origin and therefore the product  $q \frac{\partial^2 \Phi_{ax}}{\partial z^2}$  has the same value for  $\text{H}^-$  and  $\text{H}^+$ .

Then we introduce the Coulomb interaction between the ions, which we consider weak compared to the interaction with the trap potential. The system is now a pair of coupled harmonic oscillators. For small oscillations we can solve the system analytically in the context of classical mechanics (Appendix A).

The ions will exchange energy. If for instance  $H^+$  starts at rest and  $H^-$  starts with some velocity, after some time  $H^-$  will be at rest and  $H^+$  will have absorbed all of  $H^-$ 's initial kinetic energy. Then the same process happens, but in the opposite way:  $H^+$  transfers energy to  $H^-$ . And so on.

In fact, it is possible to view this process also as a series of Coulomb collisions. At each collision, a certain quantity of momentum is transferred from  $H^-$  to  $H^+$  [11]. And because they oscillate with the same frequency, the momentum transfers add up constructively.

If now we switch  $H^+$  and  $H^-$  for  $Be^+$  and  $D^-$ , the ions do not have the same mass anymore, and they will oscillate at different frequencies in their well. As a consequence, the momentum transfers cancel sometimes from one oscillation to another and the energy transfer from the hot  $D^-$  to  $Be^+$  is slower.

# Chapter 3

## Simulation code

The object of this internship is to study the sympathetic cooling of  $D^-$  with  $Be^+$  via the Coulomb interaction. Appendix A shows the derivation of the expression of the ion's positions for identical masses, without motion damping, with weak interaction and with small excursions around the rest position in one dimension. We can only provide simple analytic solutions for this case. Nonetheless, we would like to investigate the behavior of the 2-ion system beyond these approximations, and this is only made possible with a numerical simulation.

We give in this chapter an overview of the code used to simulate numerically the sympathetic cooling of  $D^-$  with  $Be^+$ . The code itself is written in Python 3.7, and we mainly used the TIQIBlitz computation unit of the TIQI Group to run the simulations.

### 3.1 Modification of CPsim

The code used for the simulations was build on an existing one called CPsim and written by Christoph Fischer, doctorate at the TIQI Group. The CPsim code is used to compute the trajectory of an ion in 3D in the presence of electric fields. Not only that, but it also proposes a framework that is able to load electric fields produced by COMSOL, as well as store the information about the ion's trajectory in a practical way. To simulate the trajectories, the code integrates the classical equation of motion of the ion:

$$m\ddot{x} = qE - \alpha\dot{x}$$

where  $\alpha$  is an optional damping coefficient.

We modified the CPsim code for our purpose, because it could only handle single-ion simulations. We extended the code to support n-ions simulations. The ions can have different properties from one to another (charge, mass, initial conditions), and interact with each other through the Coulomb interaction (in parallel of the external electric field).

We deleted the optional damping coefficient. Instead, the ions can interact through the radiation pressure with multiple laser beams, which serves as a more realistic implementation of the

ion cooling. We also added the possibility to simulate photon scattering randomly impacting the speed of the ion interacting with a laser beam.

Finally, we were also able to reduce by a factor of 30 computation times by eliminating the bottleneck of the CPsim code, which was the slow default Python interpolation code for the electric field (the electric field given as input to the code is defined only on a finite set of points in space, therefore the code interpolates linearly the value of the electric field between these points).

## 3.2 Physical model

### 3.2.1 System

#### Axial potential

We use a simplified axial potential:

$$\Phi_{ax}(x, y, z) = \frac{1}{2}U_{ax}(\alpha_{ax}z^3 + \beta_{ax}z)$$

Note that this potential does not obey the Laplace equation, but because it doesn't involve the variables  $x$  and  $y$ , it doesn't influence the ions in the radial plane, which makes it easier to study.

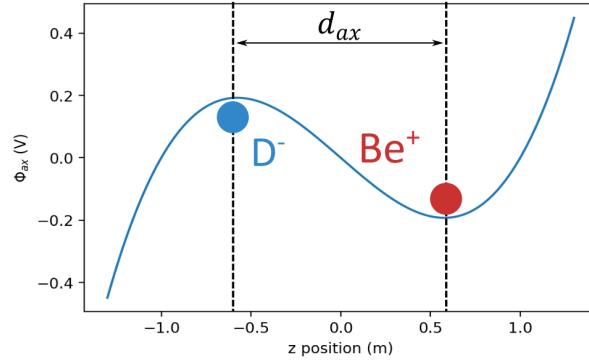


**Figure 3.1:** Plot of  $\Phi_{ax}$  as a function of  $z$  with positions of the ions in the trap.

The ion's location in the trap is shown in Fig.3.1.  $U_{ax}$  is set to 1 V. The relevant geometrical parameters of the trap are:

- the distance between the center of the wells  $d_{ax}$
- the axial trap frequency  $f_{ax}$ , which we define as the frequency of the small oscillations of an isolated  $\text{Be}^+$  ion around the center of its well along the  $z$  axis. It is related to the second derivative of  $\Phi_{ax}$  at the center of the well:

$$\Phi''_{ax}(z = d_{ax}/2) = \frac{4\pi^2 f_{ax}^2 m_{Be}}{e}$$

with  $e \simeq 1.60 \times 10^{-19}$  C and  $m_{Be} \simeq 9m_{proton} \simeq 9 \times 1.67 \times 10^{-27}$  kg.

If we settle the values of these parameters, then this determines the coefficients  $\alpha_{ax}$  and  $\beta_{ax}$  of the trap:

$$\alpha_{ax} = \frac{2\Phi''_{ax}(z = d_{ax}/2)}{3d_{ax}}$$

$$\beta_{ax} = -\frac{3}{2}\alpha_{ax}d_{ax}^2$$

### Radial potential

In the radial plane, we use an oscillating harmonic potential:

$$\Phi_{rad} = \frac{1}{2}U_{rad} \cos(\omega_{rf}t)(\alpha_{rad}x^2 - \beta_{rad}y^2)$$

$U_{rad}$  is set to 1 V. We define the radial trap frequency  $f_{rad}$  as the frequency of the small oscillations of an isolated  $D^-$  ion around the center of its well along the  $x$  axis. We calculate the coefficients:

$$\alpha_{rad} = \frac{4\pi^2 f_{rad}^2 m_D}{e}$$

$$\beta_{rad} = \frac{4\pi^2 (f_{rad} + \delta f_{rad})^2 m_D}{e}$$

with  $m_D \approx 2m_{proton} \approx 2 \times 1.67 \times 10^{-27}$  kg and  $\delta f_{rad}$  the radial trap frequency detuning between the  $x$  and  $y$  axis.

The time dependent radial potential is implemented as the time independent pseudopotential:

$$\Phi_{rad,ps} = \frac{q}{4m\omega_{rf}^2} U_{rad}^2 (\alpha_{rad}^2 x^2 + \beta_{rad}^2 y^2)$$

Note that the pseudopotential depends on the ion's mass  $m$  and charge  $q$ , therefore the ions do not feel the same radial potential.

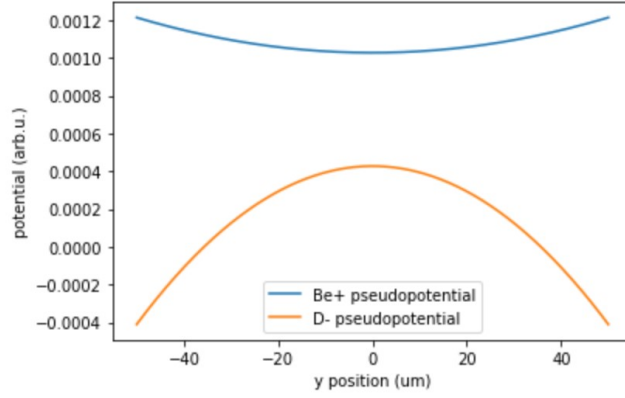


**Figure 3.2:** Plot of  $\Phi_{rad,ps}$  as a function of  $y$  for  $Be^+$  and  $D^-$  with parameters  $f_{rad} = 7$  MHz,  $\delta f_{rad} = 1$  MHz and  $\omega_{rad} = 2\pi \times 50$  MHz.

### 3.2.2 Interaction with the laser beam

#### Radiation pressure

The  $Be^+$  ion is cooled by a single laser beam at  $\lambda \approx 313.2$  nm quasi-resonant with a closed cycling transition [8] with natural linewidth  $\Gamma = 2\pi \times 19.4$  MHz. We consider that the laser emits plane-waves with wave-vector  $\mathbf{k}$ . In this approximation, the force exerted on  $Be^+$  is the radiation pressure (Appendix B):

$$\mathbf{F}_{rad} = \frac{\Gamma}{2} \frac{s}{1+s} \hbar \mathbf{k}$$

where  $s$  is the atomic saturation parameter which depends on the detuning of the laser with respect to the resonance, the orientation of the laser, the intensity of the laser and the velocity of  $Be^+$ .

Let us consider the case where  $\mathbf{v}_{Be}$  and  $\mathbf{k}$  are aligned along say the  $x$  axis. We plot  $F_{rad,x}$  (the  $x$  component of the force) as a function of  $v_{Be,x}$ .

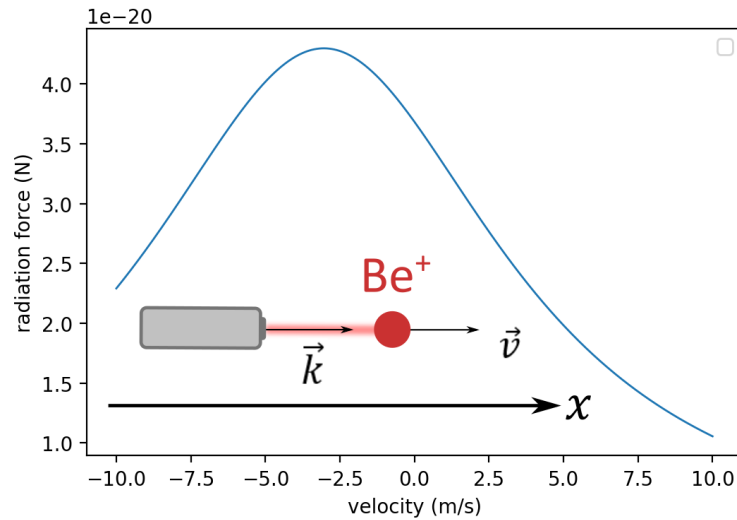


**Figure 3.3:** Plot of  $F_{rad}$  as a function of  $v_{Be}$  with illustration of the situation. Negative speed means the ion is going towards the laser.

From the plot Fig.3.3, we see that the force is always positive meaning  $Be^+$  is always pushed away from the laser. But we observe that the pushing force is stronger when the ion goes towards the laser, resulting globally in a damping of the motion if  $Be^+$  oscillates around a rest position, which is presently the case in an ion trap. This makes trapped ion cooling possible with a single laser.

In our trap, the orientation of the laser beam's wavevector  $\mathbf{k}$  is determined using spherical coordinates.

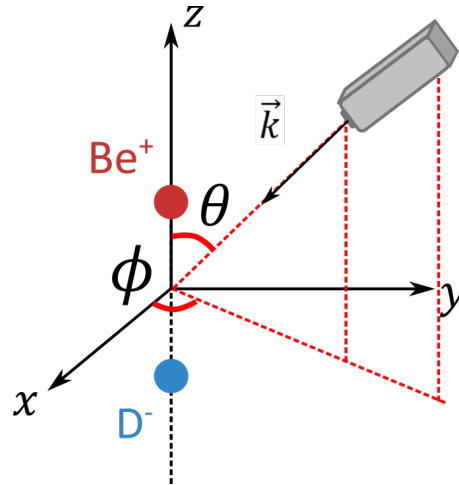


**Figure 3.4:** orientation of the laser beam is determined using spherical coordinates

### Photon scattering

A fluorescence cycle is defined as the absorption of a photon followed by its emission in a random direction of space. The number of fluorescence cycles  $Be^+$  undergoes in a second is:

$$\frac{\Gamma}{2} \frac{s}{1+s}$$

As each photon carries a momentum with value  $\hbar k \simeq 2.1 \times 10^{-27} \text{ kg m s}^{-1}$ , this translates into a random walk in momentum space for  $\text{Be}^+$  because the system  $\text{Be}^+$ +photon conserves momentum.

We implemented this effect in the code by introducing a force acting on  $\text{Be}^+$  that randomly changes the momentum of  $\text{Be}^+$  by  $\hbar k$ . In the code, the scattering events are equally spaced in time to respect the scattering rate. The axis along which each photon is emitted follows this order:  $x, y, z, x, y, z, \dots$ . The only random element in the scattering sequence is the direction in which the photon is emitted (e.g.  $+x$  or  $-x$ ). Here is an example of a scattering sequence:

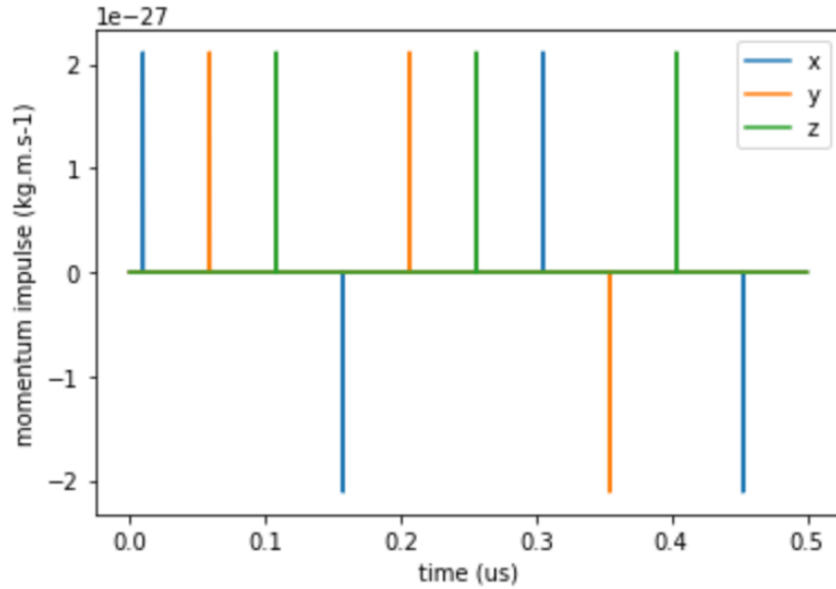


**Figure 3.5:** Scattering sequence for an atomic saturation parameter  $s = 0.5$

Strictly speaking, the scattering rate should depend on  $\text{Be}^+$ 's velocity (through the atomic saturation parameter  $s$ ), but because the sequence is generated before the integration of the equation of motion, we take the scattering rate calculated for  $\mathbf{v}_{\text{Be}} = 0$  and for a given detuning of the laser with respect to the resonance. Given the weak values of  $\mathbf{v}_{\text{Be}}$ , this approximation should not have a noticeable influence on the ion's behavior.

### 3.2.3 Equation of motion

The code integrates the following classical equation of motion:

$$m_{Be}\ddot{\mathbf{x}}_{Be} = e\mathbf{E}_{ext}(\mathbf{x}_{Be}) - \frac{e^2}{4\pi\epsilon_0} \frac{\mathbf{x}_{Be} - \mathbf{x}_D}{\|\mathbf{x}_{Be} - \mathbf{x}_D\|^3} + \frac{\Gamma}{2} \frac{s(\dot{\mathbf{x}}_{Be})}{1 + s(\dot{\mathbf{x}}_{Be})} \hbar\mathbf{k} + \mathbf{F}_{sc}$$

$$m_D\ddot{\mathbf{x}}_D = -e\mathbf{E}_{ext}(\mathbf{x}_D) + \frac{e^2}{4\pi\epsilon_0} \frac{\mathbf{x}_{Be} - \mathbf{x}_D}{\|\mathbf{x}_{Be} - \mathbf{x}_D\|^3}$$

The first term is the interaction of the ions with the electric field of the trap:

$$\mathbf{E}_{ext} = -\nabla(\Phi_{ax} + \Phi_{rad,ps})$$

The second term represents the Coulomb interaction between the ions. We use Coulomb's law even though the charges are not stationary, and neglect radiation emitted by the charges.

The term  $\frac{\Gamma}{2} \frac{s(\dot{\mathbf{x}}_{Be})}{1 + s(\dot{\mathbf{x}}_{Be})} \hbar\mathbf{k}$  in  $\text{Be}^+$ 's equation corresponds to the radiation pressure of the laser beam.

Finally,  $\mathbf{F}_{sc}$  is a force introduced to simulate the scattering of photons by  $\text{Be}^+$ .

### 3.3 Total energy

The modified CPsim code computes the trajectories of the ions. We can exploit the produced data (positions+velocities) to compute a meaningful quantity: the total energy of the system as a function of time.

The expression of the total energy is the following:

$$\mathcal{E}_{tot} = \mathcal{E}_{kin}^{Be} + \mathcal{E}_{kin}^D + \mathcal{E}_{pot}^{Be} + \mathcal{E}_{pot}^D + \mathcal{E}_{int} - \mathcal{E}_{rest}$$

We explain the different terms.

#### 3.3.1 Kinetic energy

The kinetic energy terms are straightforwardly:

$$\mathcal{E}_{kin}^{Be} = \frac{1}{2} m_{Be} \dot{\mathbf{x}}_{Be}^2$$

$$\mathcal{E}_{kin}^D = \frac{1}{2} m_D \dot{\mathbf{x}}_D^2$$

### 3.3.2 Be<sup>+</sup> potential energy

The potential energy of Be<sup>+</sup> contains two terms. The first one is due to the electric potential (Appendix C for a short note on how it is computed) and the second comes from the radiation pressure. One might object that the radiation pressure depends on the velocity of Be<sup>+</sup> and is not a conservative force for that reason. This is true, but nonetheless at order 0 the radiation pressure can be seen as a constant pushing force, and its presence displaces the rest position of Be<sup>+</sup> in the trap. Consequently, it is better to include a potential energy term arising from the radiation pressure to take into account the constant pushing.

$$\mathcal{E}_{pot}^{Be} = e \left( \Phi_{ax}(\mathbf{x}_{Be}) + \Phi_{rad,ps}^{Be}(\mathbf{x}_{Be}) \right) - \mathbf{x}_{Be} \cdot \mathbf{F}_{rad}(\dot{\mathbf{x}}_{Be} = 0)$$

### 3.3.3 D<sup>-</sup> potential energy

For D<sup>-</sup> it is the same, but without the radiation pressure:

$$\mathcal{E}_{pot}^D = -e \left( \Phi_{ax}(\mathbf{x}_D) + \Phi_{rad,ps}^D(\mathbf{x}_D) \right)$$

### 3.3.4 interaction energy

The Coulomb interaction energy between Be<sup>+</sup> and D<sup>-</sup> is:

$$\mathcal{E}_{int} = -\frac{e^2}{4\pi\epsilon_0} \frac{1}{\|\mathbf{x}_{Be} - \mathbf{x}_D\|}$$

### 3.3.5 Rest energy

In fact, all of the above terms are defined up to a constant. We can choose the constant such that the energy is zero when the system is at rest. To do so, we compute the quantity

$$\mathcal{E}_{rest} = \mathcal{E}_{pot}^{Be} + \mathcal{E}_{pot}^D + \mathcal{E}_{int}$$

by plugging in the values of the positions of the ions at rest. To compute the rest positions, we just take the average position of the ions because their movement mainly consists of oscillations around the rest position.

# Chapter 4

## Results

### 4.1 Trap stability

The cubic axial trap shape is determined by the value of the distance between the center of the wells  $d_{ax}$  and the axial trap frequency  $f_{ax}$  (reference  $\text{Be}^+$ ). However, these parameters must be chosen carefully. Indeed, for vast majority of pairs  $(d_{ax}, f_{ax})$ , the 2-ion system can decay to a stable rest state, but in some cases, the only rest state that is possible is the one where both ions sit in the center of the trap.

We can determine the stability of the trap simply by studying the rest energy of the system (Appendix A, section Rest position). Doing so, we can draw a stability map:

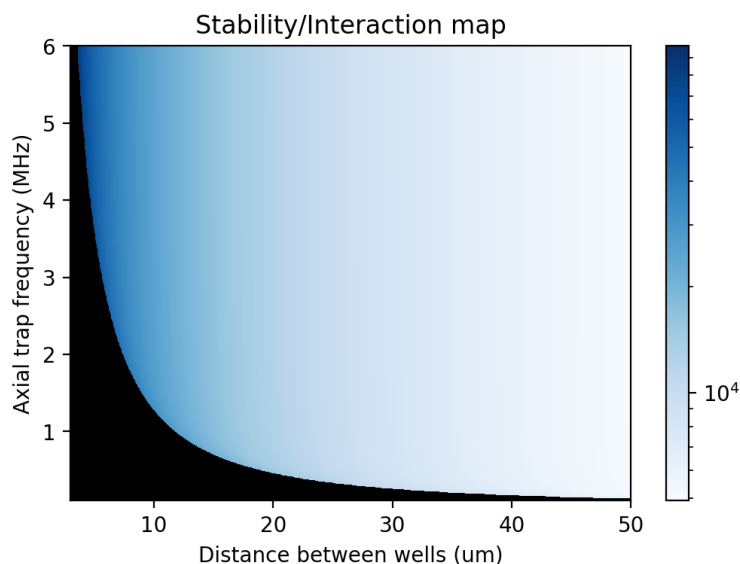


**Figure 4.1:** Stability map of the cubic ion trap. Black indicates an unstable trap, the shade of blue indicates the value of the interaction energy at rest (the Coulomb energy) in MHz.

From this we conclude that it is not possible for instance to make a trap with trap frequency 1 MHz and a distance between the wells of  $10\mu\text{m}$ .

Also, the strongest interaction between the ions at rest is found near the instability region.

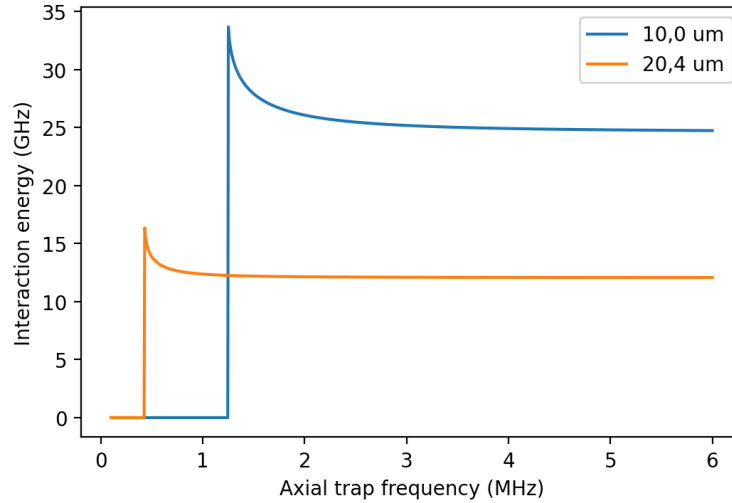


**Figure 4.2:** Interaction energy as a function of trap frequency for a fixed distance between the wells.

## 4.2 $\text{Be}^+$ laser cooling

Here we use a simple model to investigate the influence of the laser parameters on  $\text{Be}^+$ 's cooling. We put a  $\text{Be}^+$  ion in a harmonic trap. It is only allowed to move along the  $z$  axis. A laser aligned with the  $z$  axis is used to cool  $\text{Be}^+$ . The only forces acting on the ion are the electric field and the radiation pressure.

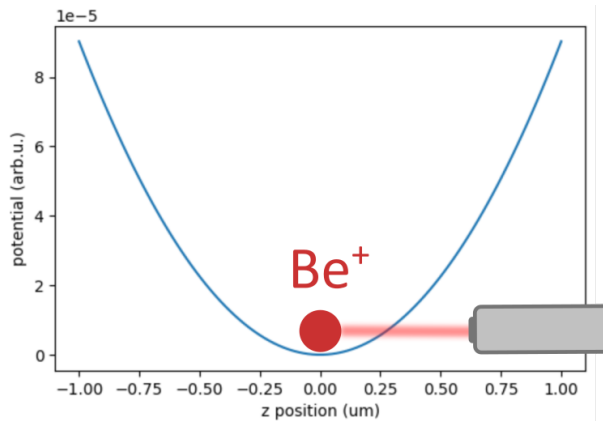


**Figure 4.3:** Drawing of the experiment

The baseline parameters are:

- initial velocity: 40 m/s
- laser wavelength: 313,2 nm
- $\text{Be}^+$  natural linewidth:  $\Gamma = 2\pi \times 19.4 \text{ MHz}$
- laser detuning with respect to the resonance:  $-\Gamma/2$
- laser saturation parameter:  $s = 0.5$
- trap frequency (reference  $\text{Be}^+$ ): 7 MHz

### 4.2.1 Trap frequency

The cooling time does not depend of the trap frequency in the MHz range:

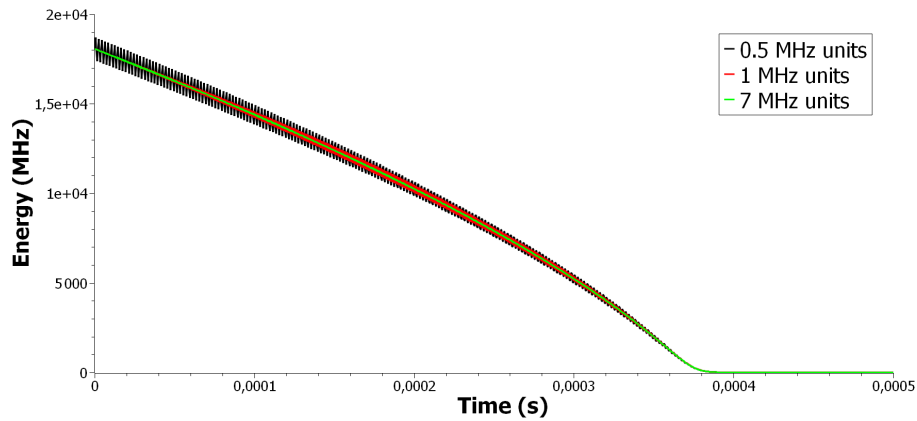


**Figure 4.4:** Total energy as a function of time for different trap frequencies

We would like to point out however that from a quantum mechanical point of view, the trap frequency is linked to the energy difference between the quantum mechanical oscillator states, and thus should affect the cooling at low energies.

### 4.2.2 Laser detuning

Let  $G = 19.4 \text{ MHz}$  ( $\text{Be}^+$  natural linewidth in Hz units). The cooling time depends strongly on the laser's detuning with respect to the resonance. The further away from resonance the laser is detuned, the faster the cooling. Starting from a certain point (Here  $-G/2 - 60 \text{ MHz}$ ), the cooling time increases however.

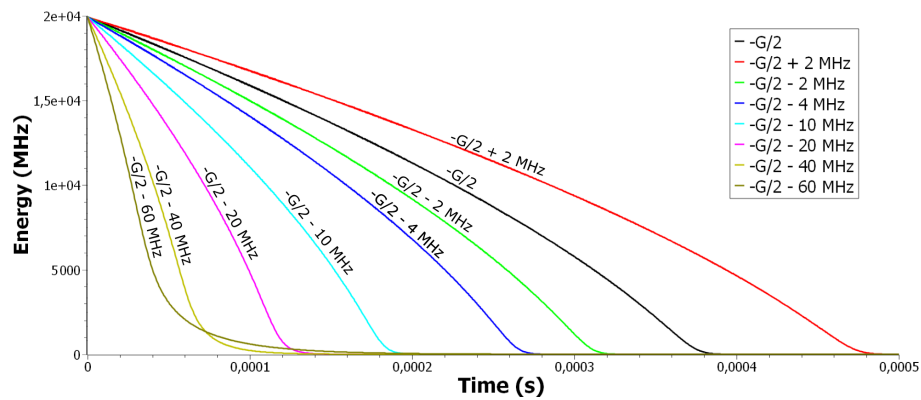


Figure 4.5: Total energy as a function of time for values of laser detuning.  $G = 19.4\text{MHz}$

Changing the trap frequency doesn't affect the detuning's effect.

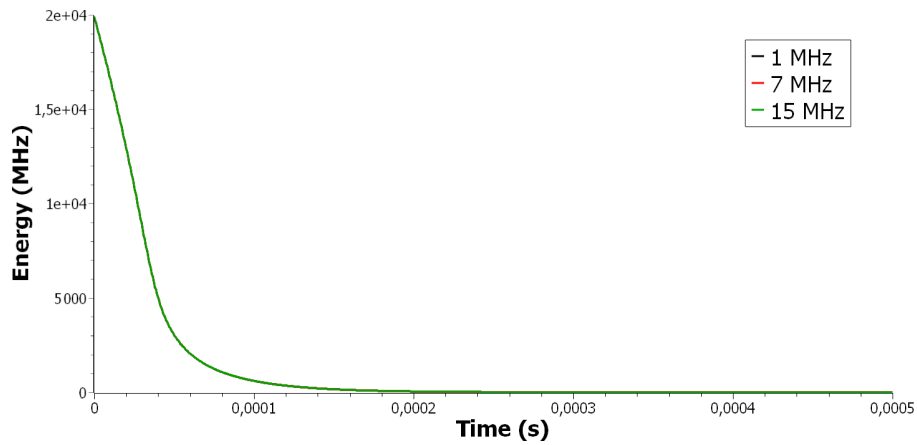
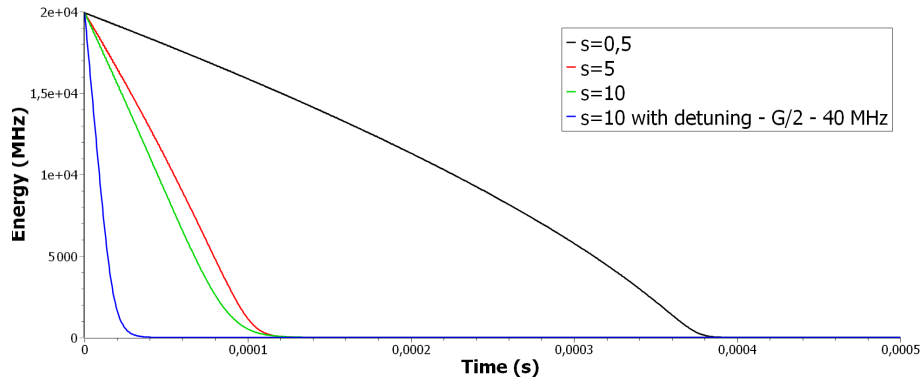


Figure 4.6: Total energy as a function of time for different trap frequencies, with the detuning set to  $-G/2 - 60\text{MHz}$ . Curves overlap.

### 4.2.3 Laser power

It is possible to speed up the cooling by increasing the laser saturation parameter. We can make it even faster by also optimizing the laser detuning, like in the previous section.



**Figure 4.7:** Total energy as a function of time for different laser saturation parameters

Note that we didn't include any effects related to photon scattering in this little experiment.

### 4.3 Sympathetic cooling

Here we study the sympathetic cooling of  $D^-$  by  $Be^+$  in the cubic trap.

#### 4.3.1 Radial trap frequency

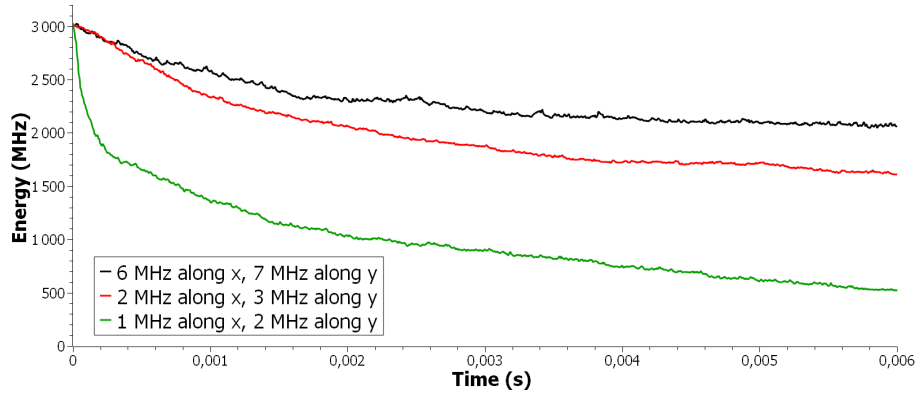


**Figure 4.8:** Total energy as a function of time for radial trap frequencies (reference  $D^-$ ). Other parameters: distance between wells:  $21\mu\text{m}$  axial trap frequency (reference  $Be^+$ ): 1 MHz; initial  $Be^+$  velocity: 20 m/s along x, y and z; laser orientation:  $\theta = 54^\circ$ ,  $\phi = 45^\circ$ ; laser detuning:  $-\Gamma/2$ ; laser saturation parameter:  $s = 0.5$

On Fig.4.8, we observe that the curve corresponding to high radial frequencies stabilizes at around 2000 MHz of energy, which is stored as kinetic and potential energy in the radial directions of  $D^-$ . To be able to cool its radial degrees of freedom as well, weak values of radial frequencies must be employed. This increases the coupling between the ions along the x and y axis.

### 4.3.2 Distance between wells

The most obvious way to reduce the cooling time is to increase the coupling between the ions, in order to increase the energy transfers between the ions. This is easily done by bringing the ions closer to each other.

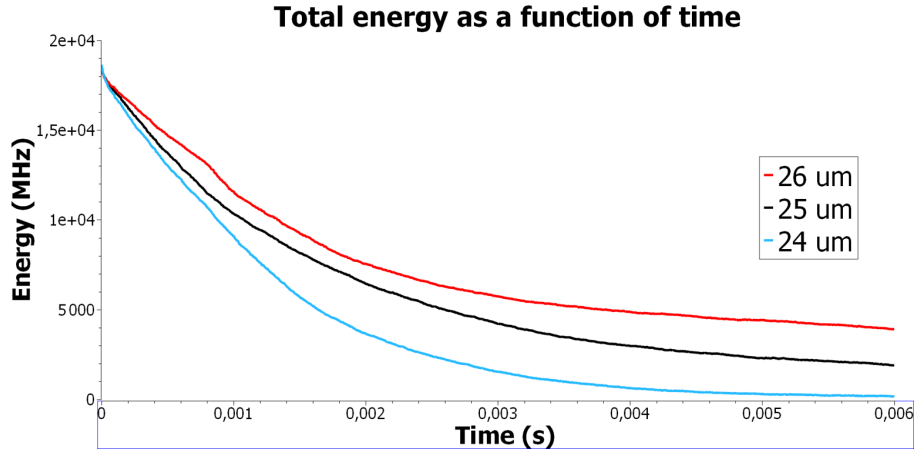


**Figure 4.9:** Total energy as a function of time for different distances between the wells. Other parameters: axial trap frequency (reference  $\text{Be}^+$ ): 1 MHz; radial trap frequencies (reference  $\text{D}^-$ ): 693 kHz along x, 905 kHz along y; initial  $\text{Be}^+$  velocity: 60 m/s along y and z; laser orientation:  $\theta = 54^\circ$ ,  $\phi = 45^\circ$ ; laser detuning:  $-\Gamma/2$ ; laser saturation parameter:  $s = 0.5$

### 4.3.3 Laser saturation parameter

The second obvious way to reduce the cooling time is to increase the laser power. However, increasing this parameter in an excessive way results in a slower cooling due to the increased photon scattering rate.

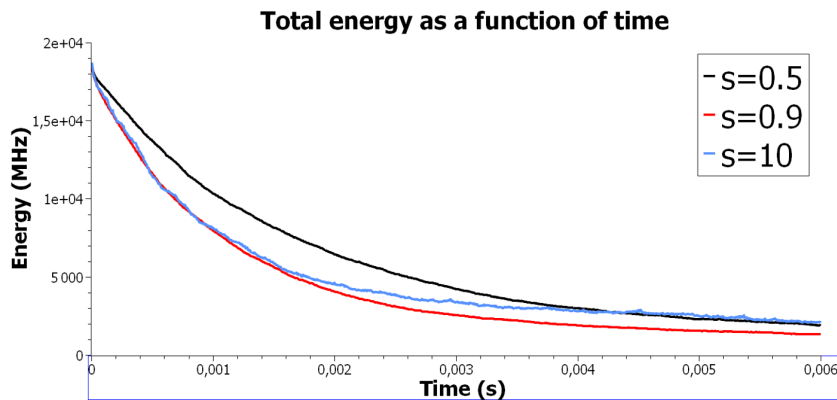


**Figure 4.10:** Total energy as a function of time for different laser saturation parameters. Other parameters: axial trap frequency (reference  $\text{Be}^+$ ): 1 MHz; distance between wells: 25  $\mu\text{m}$ ; radial trap frequencies (reference  $\text{D}^-$ ): 693 kHz along x, 905 kHz along y; initial  $\text{Be}^+$  velocity: 60 m/s along y and z; laser orientation:  $\theta = 54^\circ$ ,  $\phi = 45^\circ$ ; laser detuning:  $-\Gamma/2$ ;

#### 4.3.4 Laser detuning and orientation

It is possible to adjust the laser detuning and the laser's orientation in order to get faster cooling.

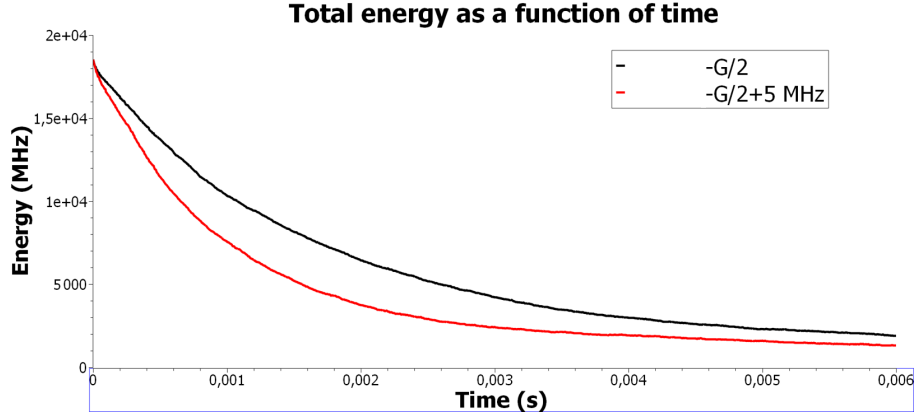


**Figure 4.11:** Total energy as a function of time for different laser detunings. Other parameters: axial trap frequency (reference  $\text{Be}^+$ ): 1 MHz; distance between wells:  $25\mu\text{m}$  radial trap frequencies (reference  $\text{D}^-$ ): 693 kHz along  $x$ , 905 kHz along  $y$ ; initial  $\text{Be}^+$  velocity: 60 m/s along  $y$  and  $z$ ; laser orientation:  $\theta = 54^\circ$ ,  $\phi = 45^\circ$ ; laser saturation parameter:  $s = 0.5$

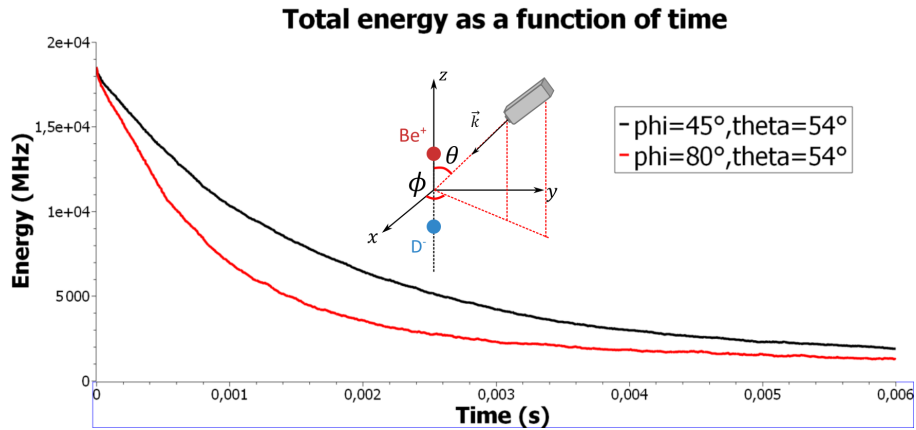


**Figure 4.12:** Total energy as a function of time for different laser orientations. Other parameters: axial trap frequency (reference  $\text{Be}^+$ ): 1 MHz; distance between wells:  $25\mu\text{m}$  radial trap frequencies (reference  $\text{D}^-$ ): 693 kHz along  $x$ , 905 kHz along  $y$ ; initial  $\text{Be}^+$  velocity: 60 m/s along  $y$  and  $z$ ; laser saturation parameter:  $s = 0.5$  laser detuning:  $-\Gamma/2$ ;

It is worth mentioning that both of these optimizations only work for weak values of radial trap frequencies. Also, only one may be applied at a time, as they mutually compensate if applied at the same time. See next section for the impact on the steady state.

### 4.3.5 Steady state

We designate by steady state the state the system reaches after a long time of exposure to the laser. Due to the photon scattering, in the steady state, the ions are still in movement, but very closely to their rest position. We measure the average energy of the steady state by letting the system evolve when the ions start at rest near their rest position.

The laser saturation parameter has an impact on the average energy of the rest state.

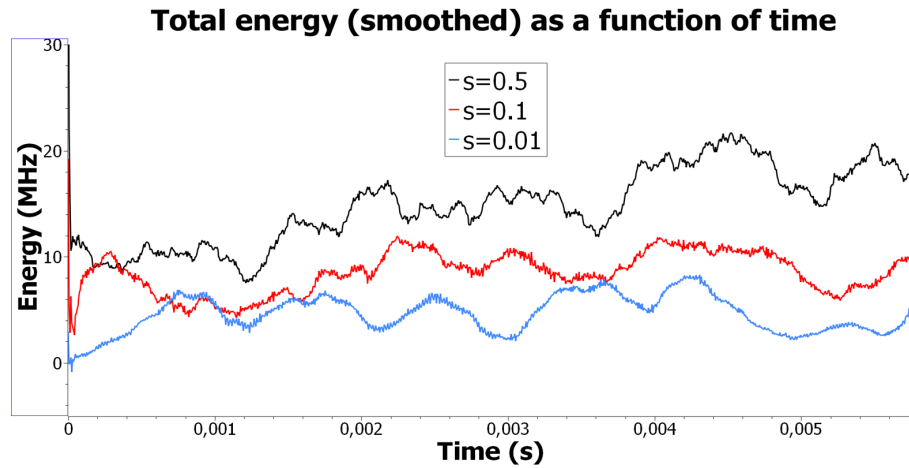


**Figure 4.13:** Total energy as a function of time for different laser saturation parameters, with the ions starting at rest near their rest position. The curves have been smoothed using a moving average. Other parameters: axial trap frequency (reference  $\text{Be}^+$ ): 1 MHz; distance between wells:  $25\mu\text{m}$  radial trap frequencies (reference  $\text{D}^-$ ): 693 kHz along  $x$ , 905 kHz along  $y$ ; laser orientation:  $\theta = 54^\circ$ ,  $\phi = 45^\circ$ ; laser detuning:  $-\Gamma/2$ ;

Also, using the optimized laser detuning or orientation from the above subsection results in a higher average total energy.

## Temperature

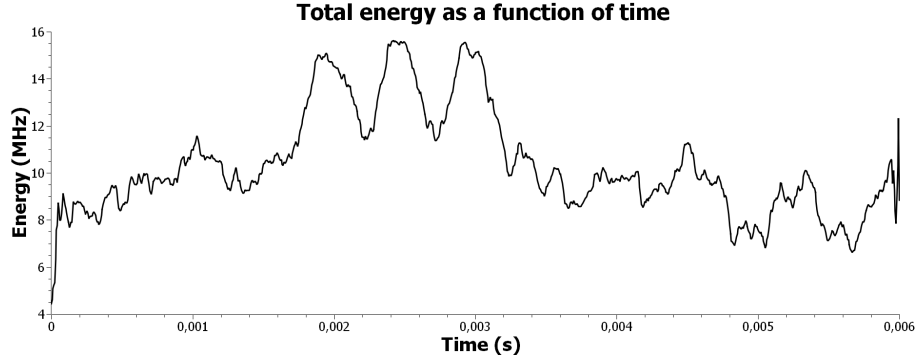


**Figure 4.14:** Total energy as a function of time with the ions starting at rest near their rest position. The curve has been smoothed using a moving average. Other parameters: axial trap frequency (reference  $\text{Be}^+$ ): 1,02 MHz; distance between wells:  $20.86\mu\text{m}$  radial trap frequencies (reference  $\text{D}^-$ ): 6,395 MHz along  $x$ , 6,855 MHz along  $y$ ; laser saturation parameter:  $s = 0.5$ ; laser orientation:  $\theta = 54^\circ$ ,  $\phi = 45^\circ$ ; laser detuning:  $-\Gamma/2$ ;

Using the parameters of Fig.4.14, the average velocity of the ions is 0,56 m/s for  $\text{Be}^+$  and 0,52 m/s for  $\text{D}^-$ , which corresponds to:

$$T_{\text{Be}} = 114\mu\text{K}$$

$$T_{\text{D}} = 22\mu\text{K}$$

### 4.3.6 Comparison with a more realistic electric field

In this subsection, we compare the sympathetic cooling of the 2-ion system in our simplified cubic trap with a more realistic trap produced by COMSOL (it obeys Maxwell's equations, so the axial trap will be anti-confining in some direction). We converted the COMSOL radial trap into a pseudopotential.

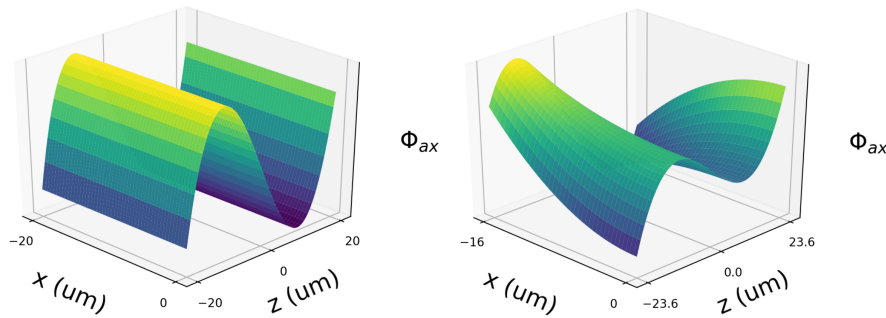


**Figure 4.15:** (Left) Simplified axial trap as a function of  $x$  and  $z$ . (Right) Realistic axial trap as a function of  $x$  and  $z$ . We clearly see the anti-confining character along the  $x$  axis.

In order to compare these traps, we tailor our simplified trap to look similar to the real trap by setting carefully chosen values for the following parameters:

- Axial trap frequency (reference  $\text{Be}^+$ ): 1,02 MHz
- Distance between wells:  $20.86\mu\text{m}$
- Radial trap frequency in the (x+y) direction (reference  $\text{D}^-$ ) (along the bisector of  $\mathbf{e}_x$  and  $\mathbf{e}_y$ ): 6,395 MHz
- Radial trap frequency in the (x-y) direction (reference  $\text{D}^-$ ) (along the bisector of  $\mathbf{e}_x$  and  $-\mathbf{e}_y$ ): 6,855 MHz

Setting these parameters for the simplified trap, we find the traps to be visually very similar along the z axis.

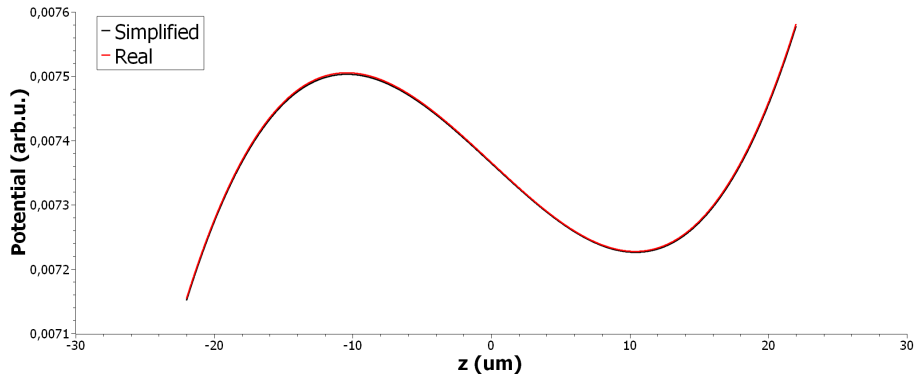


**Figure 4.16:** Plot of axial potentials as a function of  $z$

It is worth noting that with these parameters, the frequency of the oscillations of an isolated  $\text{D}^-$  in the (x+y) and (x-y) direction are the same in the simplified trap and in the realistic trap. However there are some discrepancies for the frequency of the oscillations of an isolated  $\text{Be}^+$ :

- (x+y) direction: 1,035 MHz in the realistic trap and 1,42 MHz in the simplified one.
- (x-y) direction: 1,56 MHz in the realistic trap and 1,52 MHz in the simplified one.

These are explained by the anti-confinement in the radial plane of the axial trap.

Running simulations in the simplified trap and in the realistic trap with the same initial conditions, we get:

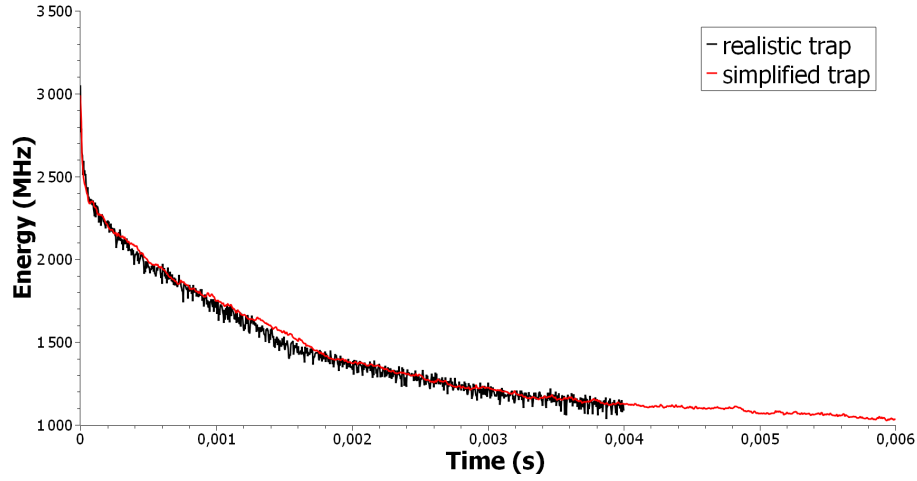


**Figure 4.17:** Plot of the total energy as a function of time. Ions start at the bottom of their well ( $\pm 10.43 \mu\text{m}$ ) and  $D^-$  starts with  $v_y = v_z = 20 \text{ m/s}$

The curves overlap quite well, meaning our results with the simulations in the simplified trap must also hold for more realistic traps. We notice however that the total energy curve for the realistic trap is more jagged. This has no physical origin and is due to the method we use to compute the electric potential (see Appendix C).

In Fig.4.17, after 6 ms, there are 1000 MHz of energy left in the system. They are much more difficult to extract because of the high radial trap frequency. We should therefore lower the radial trap's voltage. For the experiment done here it was set to 52 V. We could lower the voltage to 40 V and still keep the ions in the trap, which resulted in radial trap frequencies (reference  $D^-$ ) of 4,7 MHz along the (x+y) direction and 5,3 MHz along the (x-y) one. Our study of the impact of the radial trap frequency on the cooling suggests that it isn't low enough, and indeed,  $D^-$  energy still can't be fully evacuated.

### 4.3.7 Trap modulation

To cool the system faster, we tried modulating the axial trap. Examples of modulations are:

$$\begin{aligned}\Phi_{ax}(x, y, z, t) &= \frac{1}{2}U_{ax}\left(\alpha_{ax}z^3 + \beta_{ax}[1 + \epsilon_1 \cos(\omega_{mod} t)]z\right) \\ \Phi_{ax}(x, y, z, t) &= \frac{1}{2}U_{ax}\left(\alpha_{ax}z^3 + \alpha_{ax}\epsilon_2 \cos(\omega_{mod} t)z^2 + \beta_{ax}z\right) \\ \Phi_{ax}(x, y, z, t) &= \frac{1}{2}U_{ax}\left(\alpha_{ax}[1 + \epsilon_3 \cos(\omega_{mod} t)]z^3 + \beta_{ax}z\right)\end{aligned}$$

with  $\omega_{mod} = 2\pi\Delta f$ , where  $\Delta f = \left(\sqrt{\frac{9}{2}} - 1\right) f_{ax}$  is the difference of axial secular motion frequencies for  $\text{Be}^+$  and  $D^-$ .

However, experiments didn't show any improvements in the cooling time when applying a modulation on the axial trap.

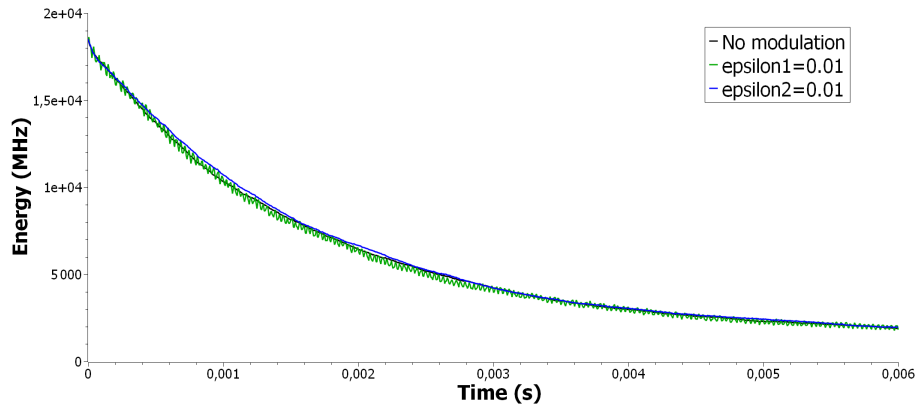


**Figure 4.18:** Plot of the total energy as a function of time when applying 2 types of modulations.

Modulating the quadratic radial potential at the difference of secular motion frequencies along one axis didn't help either to eliminate the remaining  $D^-$  energy in the radial plane.

A possible solution that could be used to overcome the need for low radial frequencies to eliminate radial kinetic energy would be to be able to couple the axial degree of freedom with the radial ones, which could be achieved using another type of modulation [12].

## Chapter 5

# Discussion and Conclusion

**Trap stability** We showed that not all cubic axial trap geometries permit the ( $D^- + Be^+$ ) system to decay towards a stable configuration. It can happen that the attraction between the ions is stronger than the trap keeping them apart from each other. Thus, this situation is radically different from the already experimentally tested trapped 2-cation systems, and this constraint will need to be mastered when manipulating cation-anion systems in miniaturized trap arrays for quantum computing.

**Be+ laser cooling** We confirmed in this section a few characteristics of ion cooling that are experimentally observed, notably the fact that the cooling does not depend on the value of the trap frequency (for a perfectly harmonic trap) and that large negative values of laser detuning speed up the cooling. We studied also the effect of increased laser power and observed that it decreases the cooling time, however we did not include effects to the scattering of photons to keep this experiment simple.

**Sympathetic cooling: radial trap frequency** We showed that in the context of sympathetic cooling, the trap frequency of the radial trap is an important parameter: if the radial trap frequency is too high, the coupling between the ions in the radial plane become very weak. As a result, the energy stored by  $D^-$  in the radial plane can't be transferred to  $Be^+$ . Reducing the radial trap frequency solves the problem, however this solution can't be applied to real traps, where the axial trap is anti-confining in the radial plane: in order to reduce the radial trap frequency, the voltage of the radial trap has to be decreased, which means the ions are more easily ejected from the trap (the heavier  $Be^+$  in particular). One way to circumvent this limitation would be to be able to transfer the radial energy of  $D^-$  to its axial energy, using a type of trap modulation [12].

**Sympathetic cooling: distance between the ions** We showed that, for low radial trap frequencies, the 2-ion system can be cooled in a reasonable amount of times (6 ms for starting velocities of 60 m/s along the y and z axes). We observed that it is possible to increase the cooling rate by bringing the ions closer to each other. The bottleneck of the sympathetic cooling process being the energy transfer from  $D^-$  to  $Be^+$ , it makes sense that the parameter with the most impact on the cooling time is the separation distance between the ions, as bringing them closer to each other increases the coupling, which in turn increases the energy transfers. We tried also to increase the

coupling by applying trap modulations, but we didn't find the modulation to change anything to the cooling's behavior.

**Sympathetic cooling: parameters acting on  $\text{Be}^+$**  We found that acting on  $\text{Be}^+$  can impact the cooling. Increasing the laser power increases the cooling rate up to a certain point, because the energy is evacuated faster from the system. Increasing too much the laser power, increases the photon scattering rate as well, which hinders the cooling. Other parameters include the laser orientation and the laser detuning, but the effect of these parameters is not understood.

## Conclusion

The use of different ions species in the context of quantum technologies, like quantum logic spectroscopy or quantum computing, could offer new possibilities in contrast to same-ion systems. Before being able to use the ions as quantum systems, they need to be cooled down. Our motivations for this internship are to investigate if the sympathetic cooling of a hot  $\text{D}^-$  by a  $\text{Be}^+$  held cold by laser cooling is possible and which parameters are the most relevant during this process.

The results of the simulation show that cooling  $\text{D}^-$  by  $\text{Be}^+$  is possible when the radial trap frequency is sufficiently low, and the cooling rate is higher if the ions are brought closer to each other in the ion trap, and if the laser power is more intense (up to a certain limit). Other parameters influencing the cooling time include the laser detuning and orientation. Finally, we compared the behavior of the cooling in simplified traps and in more realistic traps, with results closely matching.

The mentioned results are fairly general and should apply to other systems than ( $\text{D}^- + \text{Be}^+$ ), like (anti-proton +  $\text{Be}^+$ ) for instance.

# **Appendices**

## Appendix A

# Coupled harmonic oscillators in the cubic trap

### A.1 Presentation of the system

We have a  $H^+$  cation and a  $H^-$  anion in the following potential:

$$\Phi_{ax}(x, y, z) = \frac{1}{2} U_{ax} (\alpha_{ax} z^3 + \beta_{ax} z) + f(x, y) \quad \alpha_{ax} > 0, \beta_{ax} < 0$$

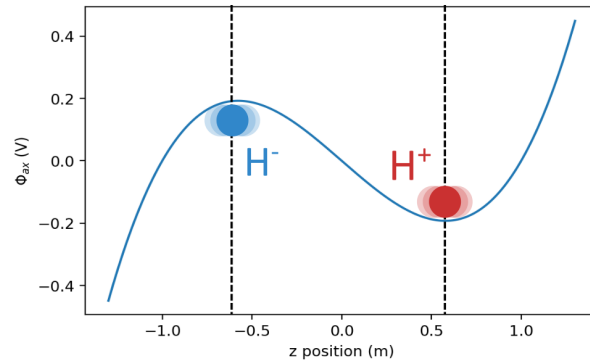


**Figure A.1:** Configuration of the system. Dashed lines represent the local extrema of  $\Phi_{ax}$  along the  $z$  axis.  $\alpha_{ax} = 1 \text{ m}^{-3}$  and  $\beta_{ax} = -1 \text{ m}^{-1}$

The ions move only along the  $z$  axis and therefore we do not introduce a radial confinement potential. Only small oscillations around the rest position are permitted. The  $z$  position of  $H^+$  is labeled  $z_+$  and the one of  $H^-$  is labeled  $z_-$ . The local extrema of  $\Phi_{ax}$  along the  $z$  axis (bottom of  $H^+$  well and top of  $H^-$  hill) are located at:

$$z = \pm \frac{\beta_{ax}}{3\alpha_{ax}}$$

## A.2 Lagrangian of the system

In our cartesian coordinate system attached to the reference frame of the laboratory, the Lagrangian  $\mathcal{L}$  is simply the kinetic energy minus the potential energy (electric potential + Coulomb interaction).

We have therefore:

$$\mathcal{L} = \mathcal{E}_{kin} - \mathcal{E}_{pot} - \mathcal{E}_{int}$$

with

$$\mathcal{E}_{kin} = \frac{1}{2} m \dot{z}_+^2 + \frac{1}{2} m \dot{z}_-^2$$

$$\mathcal{E}_{pot} = e\Phi_{ax}(z_+) - e\Phi_{ax}(z_-)$$

$$\mathcal{E}_{int} = -\frac{e^2}{4\pi\epsilon_0} \frac{1}{z_+ - z_-}$$

## A.3 Rest position

If the Coulomb interaction didn't exist, the rest position of  $H^+$  would be the bottom of its well and the rest position of  $H^-$  would be the top of its hill (local extrema of the trap along the  $z$  axis). But because they attract each other, in reality the rest position is a bit different.

The shift in the rest positions can be computed. At rest, the total energy of the system is simply:

$$\mathcal{E}_{rest} = \mathcal{E}_{pot} + \mathcal{E}_{int} = e\Phi_{ax}(z_+) - e\Phi_{ax}(z_-) - \frac{e^2}{4\pi\epsilon_0} \frac{1}{z_+ - z_-}$$

Because of the symmetry of the axial potential, at rest we have  $z_+ = -z_- = z_0$  which simplifies the expression above:

$$\mathcal{E}_{rest}(z_0) = e\Phi_{ax}(z_0) - e\Phi_{ax}(-z_0) - \frac{e^2}{8\pi\epsilon_0 z_0}$$

The equilibrium position of the system corresponds to local minimum of the rest total energy, meaning:

$$\frac{d\mathcal{E}_{rest}}{dz_0}(z_0) = 0 \Leftrightarrow z_0^4 + \frac{\beta_{ax}}{3\alpha_{ax}} z_0^2 + \frac{e}{24\pi\epsilon_0 U_{ax} \alpha_{ax}} = 0$$

This is a quadratic equation in  $z_0^2$  with discriminant:

$$\Delta = \left( \frac{\beta_{ax}}{3\alpha_{ax}} \right)^2 - \frac{e}{6\pi\epsilon_0 U_{ax} \alpha_{ax}}$$

If  $\Delta < 0$ , then there are no real solutions to this equation, which means the system will simply collapse because the ions attract each other stronger than what the trap can keep them apart. We will assume that the following condition is satisfied:

$$\Delta > 0 \Leftrightarrow \beta_{ax}^2 > \frac{3e\alpha_{ax}}{2\pi\epsilon_0 U_{ax}}$$

The solution of the quadratic equation is (we keep only the positive one):

$$z_0^2 = \frac{-\frac{\beta_{ax}}{3\alpha_{ax}} + \sqrt{\Delta}}{2} \Rightarrow z_0 = \sqrt{\frac{-\frac{\beta_{ax}}{3\alpha_{ax}} + \sqrt{\Delta}}{2}}$$

We can plot the rest position as a function of the voltage applied  $U_{ax}$ .

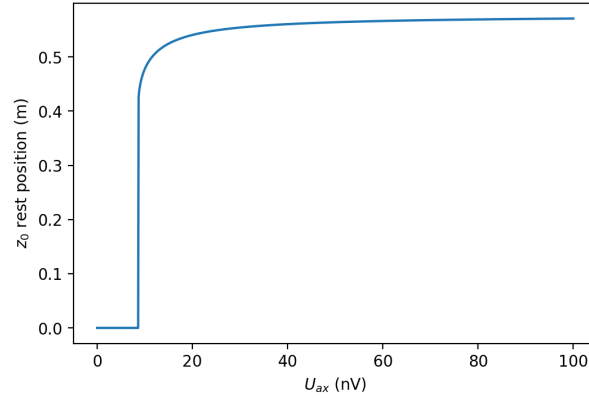


**Figure A.2:** Plot of  $z_0$  as a function of  $U_{ax}$  for  $\alpha_{ax} = 1 \text{ m}^{-3}$  and  $\beta_{ax} = -1 \text{ m}^{-1}$

We see that for a weak attraction between the ions compared to  $e\Phi_{ax}$  (ie. when we turn up the voltage  $U_{ax}$  of the trap), the rest positions corresponds to the local minima of the trap.

$$z_0 \sim -\frac{\beta_{ax}}{3\alpha_{ax}} > 0 \quad \text{when} \quad U_{ax} \longrightarrow \infty$$

From now on we will consider that the attraction between the ions is weak compared to  $e\Phi_{ax}$ . The rest positions of the ions corresponds to the local minima of the trap in this approximation, which have the property that the derivative of the potential along  $z$  is zero at these points:

$$\frac{\partial \Phi_{ax}}{\partial z}(z = z_0) = 0$$

## A.4 Taylor expansion of the Lagrangian

We consider that the ions move very closely to their rest position:

$$z_+ = z_0 + \varepsilon_+$$

$$z_- = -z_0 + \varepsilon_-$$

$$z_0 = -\frac{\beta_{ax}}{3\alpha_{ax}} > 0$$

The kinetic energy can be written:

$$\mathcal{E}_{kin} = \frac{1}{2}m\dot{\varepsilon}_+^2 + \frac{1}{2}m\dot{\varepsilon}_-^2$$

### A.4.1 Electric potential energy

$$\mathcal{E}_{pot} = e\Phi_{ax}(z_+) - e\Phi_{ax}(z_-)$$

We have:

$$\Phi_{ax}(z_+) \sim \Phi_{ax}(z_0) + \varepsilon\Phi'_{ax}(z_0) + \frac{\varepsilon^2}{2}\Phi''_{ax}(z_0)$$

From now on we will forget about constant terms in the energies to simplify the expressions without changing the physics. Also, because  $z_0$  corresponds to a local minimum of  $\Phi_{ax}$ , we have  $\Phi'_{ax}(z_0) = 0$  and we can write:

$$\Phi_{ax}(z_+) \sim \frac{\varepsilon_+^2}{2}\Phi''_{ax}(z_0)$$

$$\mathcal{E}_{pot} \sim e\frac{\varepsilon_+^2}{2}\Phi''_{ax}(z_0) - e\frac{\varepsilon_-^2}{2}\Phi''_{ax}(-z_0)$$

Using the symmetry of the trap, we can further simplify the expression of the trap by noting that

$$\Phi''_{ax}(z_0) = -\Phi''_{ax}(-z_0)$$

and we get:

$$\mathcal{E}_{pot} \sim e\Phi''_{ax}(z_0)(\varepsilon_+^2 + \varepsilon_-^2)$$

### A.4.2 Interaction energy

$$\mathcal{E}_{int} = -\frac{e^2}{4\pi\epsilon_0} \frac{1}{z_+ - z_-}$$

The Taylor expansion here is straightforward:

$$\mathcal{E}_{int} \sim -\frac{e^2}{4\pi\epsilon_0} \left( \frac{1}{2z_0} - \frac{\epsilon_+ - \epsilon_-}{4z_0^2} + \frac{(\epsilon_+ - \epsilon_-)^2}{8z_0^3} \right)$$

The first term is constant. The second term only induces a constant change in the rest position of the ions, which is physically uninteresting. Both terms are dumped and so we have:

$$\mathcal{E}_{int} \sim -\frac{e^2}{32\pi\epsilon_0 z_0^3} (\epsilon_+ - \epsilon_-)^2$$

### A.4.3 Lagrangian

Using the simplified expressions for the energies:

$$\mathcal{L}(\epsilon_+, \epsilon_-, \dot{\epsilon}_+, \dot{\epsilon}_-) \sim \frac{1}{2} m \dot{\epsilon}_+^2 + \frac{1}{2} m \dot{\epsilon}_-^2 - e\Phi''_{ax}(z_0)(\epsilon_+^2 + \epsilon_-^2) + \frac{e^2}{32\pi\epsilon_0 z_0^3} (\epsilon_+ - \epsilon_-)^2$$

We introduce the following parameters, which can be considered as generalized spring constants:

$$k_{pot} = 2e\Phi''_{ax}(z_0)$$

$$k_{int} = \frac{e^2}{16\pi\epsilon_0 z_0^3}$$

yielding:

$$\mathcal{L}(\epsilon_+, \epsilon_-, \dot{\epsilon}_+, \dot{\epsilon}_-) \sim \frac{1}{2} m \dot{\epsilon}_+^2 + \frac{1}{2} m \dot{\epsilon}_-^2 - \frac{k_{pot}}{2} (\epsilon_+^2 + \epsilon_-^2) + \frac{k_{int}}{2} (\epsilon_+ - \epsilon_-)^2$$

## A.5 Hamiltonian

We wish to transition to the Hamiltonian formalism. We compute to that end the generalized momenta:

$$p_+ = \frac{\partial \mathcal{L}}{\partial \dot{\epsilon}_+} = m \dot{\epsilon}_+$$

$$p_- = \frac{\partial \mathcal{L}}{\partial \dot{\epsilon}_-} = m \dot{\epsilon}_-$$

and we can write:

$$\mathcal{H}(\varepsilon_+, \varepsilon_-, p_+, p_-) \sim \frac{1}{2m} p_+^2 + \frac{1}{2m} p_-^2 + \frac{k_{pot}}{2} (\varepsilon_+^2 + \varepsilon_-^2) - \frac{k_{int}}{2} (\varepsilon_+ - \varepsilon_-)^2$$

## A.6 Equations of motion

Hamilton's equations are:

$$\dot{p}_+ = -\frac{\partial \mathcal{H}}{\partial \varepsilon_+} \quad \dot{p}_- = -\frac{\partial \mathcal{H}}{\partial \varepsilon_-}$$

which yield:

$$\begin{aligned} \ddot{\varepsilon}_+ + \frac{k_{pot} - k_{int}}{m} \varepsilon_+ &= -\frac{k_{int}}{m} \varepsilon_- \\ \ddot{\varepsilon}_- + \frac{k_{pot} - k_{int}}{m} \varepsilon_- &= -\frac{k_{int}}{m} \varepsilon_+ \end{aligned}$$

Instead of solving these coupled equations, we let:

$$\varepsilon_s = \frac{\varepsilon_+ + \varepsilon_-}{2} \quad \varepsilon_a = \frac{\varepsilon_+ - \varepsilon_-}{2}$$

It follows that:

$$\begin{aligned} \ddot{\varepsilon}_s + \frac{k_{pot}}{m} \varepsilon_s &= 0 \\ \ddot{\varepsilon}_a + \frac{k_{pot} - 2k_{int}}{m} \varepsilon_a &= 0 \end{aligned}$$

The general solution to these uncoupled equations is:

$$\begin{aligned} \varepsilon_s &= A \cos \left( \sqrt{\frac{k_{pot}}{m}} t \right) + B \sin \left( \sqrt{\frac{k_{pot}}{m}} t \right) \\ \varepsilon_a &= C \cos \left( \sqrt{\frac{k_{pot} - 2k_{int}}{m}} t \right) + D \sin \left( \sqrt{\frac{k_{pot} - 2k_{int}}{m}} t \right) \end{aligned}$$

## A.7 Initial conditions

The initial conditions are for  $t = 0$ :

$$\begin{aligned}\varepsilon_+(0) &= 0 \\ \varepsilon_-(0) &= 0 \\ \dot{\varepsilon}_+(0) &= 0 \\ \dot{\varepsilon}_-(0) &= v_0 \in \mathbb{R}\end{aligned}$$

which translate into the following initial conditions for  $\varepsilon_s$  and  $\varepsilon_a$ :

$$\begin{aligned}\varepsilon_s(0) &= 0 \\ \varepsilon_a(0) &= 0 \\ \dot{\varepsilon}_s(0) &= v_0/2 \\ \dot{\varepsilon}_a(0) &= -v_0/2\end{aligned}$$

meaning:

$$\begin{aligned}\varepsilon_s &= \frac{v_0}{2} \sqrt{\frac{m}{k_{pot}}} \sin\left(\sqrt{\frac{k_{pot}}{m}} t\right) \\ \varepsilon_a &= \frac{v_0}{2} \sqrt{\frac{m}{k_{pot} - 2k_{int}}} \sin\left(\sqrt{\frac{k_{pot} - 2k_{int}}{m}} t\right)\end{aligned}$$

We go back to  $\varepsilon_+ = \varepsilon_s + \varepsilon_a$  and  $\varepsilon_- = \varepsilon_s - \varepsilon_a$ :

$$\begin{aligned}\varepsilon_+ &= \frac{v_0}{2} \sqrt{\frac{m}{k_{pot}}} \sin\left(\sqrt{\frac{k_{pot}}{m}} t\right) + \frac{v_0}{2} \sqrt{\frac{m}{k_{pot} - 2k_{int}}} \sin\left(\sqrt{\frac{k_{pot} - 2k_{int}}{m}} t\right) \\ \varepsilon_- &= \frac{v_0}{2} \sqrt{\frac{m}{k_{pot}}} \sin\left(\sqrt{\frac{k_{pot}}{m}} t\right) - \frac{v_0}{2} \sqrt{\frac{m}{k_{pot} - 2k_{int}}} \sin\left(\sqrt{\frac{k_{pot} - 2k_{int}}{m}} t\right)\end{aligned}$$

We plot the solutions as functions of time.

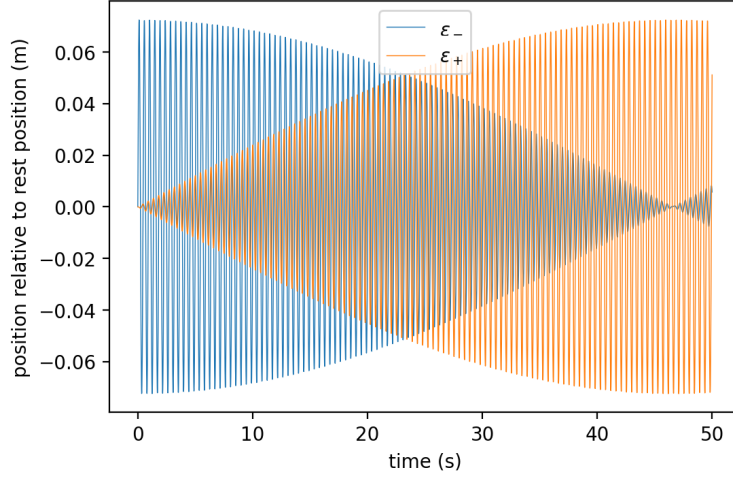


**Figure A.3:**  $\varepsilon_+$  and  $\varepsilon_-$  as functions of time for  $v_0 = 1 \text{ m/s}$ ,  $\alpha_{ax} = 1 \text{ m}^{-3}$ ,  $\beta_{ax} = -1 \text{ m}^{-1}$  and  $U_{ax} = 1 \mu\text{V}$ .

## A.8 Beating

On the plot Fig.A.3, we see that  $H^-$  and  $H^+$  follow a beating motion. Also,  $H^-$  transfers the totality of its initial kinetic energy to  $H^+$  in about 46,5 s. The beating motion does not appear immediately from the analytic expressions of  $\varepsilon_+$  and  $\varepsilon_-$ . However, if we notice that  $k_{int} \ll k_{pot}$  because the interaction between the ions is weak:

$$\varepsilon_+ \simeq \frac{v_0}{2} \sqrt{\frac{m}{k_{pot}}} \left[ \sin\left(\sqrt{\frac{k_{pot}}{m}} t\right) + \sin\left(\sqrt{\frac{k_{pot} - 2k_{int}}{m}} t\right) \right]$$

$$\varepsilon_- \simeq \frac{v_0}{2} \sqrt{\frac{m}{k_{pot}}} \left[ \sin\left(\sqrt{\frac{k_{pot}}{m}} t\right) - \sin\left(\sqrt{\frac{k_{pot} - 2k_{int}}{m}} t\right) \right]$$

$\varepsilon_+$  and  $\varepsilon_-$  are a superposition of two sines of very close frequencies:

$$f_1 = \frac{1}{2\pi} \sqrt{\frac{k_{pot}}{m}}$$

$$f_2 = \frac{1}{2\pi} \sqrt{\frac{k_{pot} - 2k_{int}}{m}} \sim \frac{1}{2\pi} \sqrt{\frac{k_{pot}}{m}} \left(1 - \frac{k_{int}}{k_{pot}}\right)$$

The positions of the ions oscillate a frequency  $f_1 + f_2$ , but the envelope of the positions varies with a frequency:

$$|f_1 - f_2| = \frac{1}{2\pi} \frac{k_{int}}{\sqrt{mk_{pos}}}$$

## A.9 Damping

Now we consider that the motion of  $H^+$  is damped. If the damping is sufficiently strong, we can expect the system to reach its rest state after half an oscillation of the beating's envelope, that is when  $H^+$  has absorbed all of  $H^-$ 's initial kinetic energy in the previous situation (it corresponds here to about 46,5 s).

The equations of motion are now:

$$\begin{aligned} \ddot{\epsilon}_+ + \frac{\gamma}{m} \dot{\epsilon}_+ + \frac{k_{pot} - k_{int}}{m} \epsilon_+ &= -\frac{k_{int}}{m} \epsilon_- \\ \ddot{\epsilon}_- + \frac{k_{pot} - k_{int}}{m} \epsilon_- &= -\frac{k_{int}}{m} \epsilon_+ \end{aligned}$$

with  $\gamma$  the damping coefficient.

Because there are no simple analytic solutions, we integrate the equation of motion numerically to obtain:

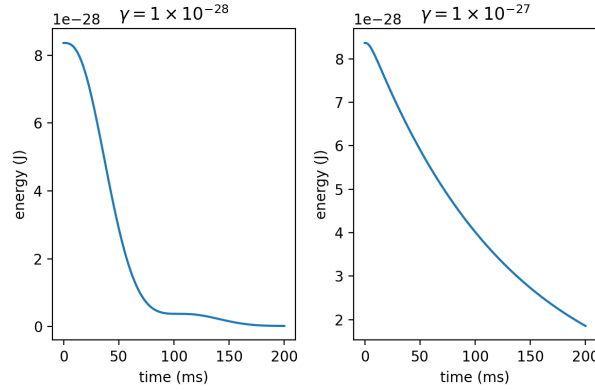


**Figure A.4:** Total energy as a function of time for different values of the damping coefficient.  $\alpha_{ax} = -1 \text{ m}^{-3}$ ;  $\beta_{ax} = 1 \text{ m}^{-1}$  and  $U_{ax} = 1 \text{ V}$ .

It is more insightful to plot the total energy of the system as a function of time. We observe that the system takes more time to cool down than the expected 46,5 s, and also increasing too much the damping coefficient will starting from a certain point increase as well the cooling time. This makes actually sense, because if  $H^+$  was motionless, no energy could be transferred from  $H^-$  to  $H^+$ .

## Appendix B

# Laser manipulation of atoms

Here we explain the theory behind the model used for the interaction of  $\text{Be}^+$  with the cooling laser. Consider an atom with velocity  $\boldsymbol{v}$ . We shine a laser on the atom, that is quasi-resonant with the atomic transition between the internal states  $|1\rangle$  and  $|2\rangle$  separated by  $\Delta\mathcal{E} = \hbar\omega_0$ . We suppose that the laser emits plane waves of the form:

$$\boldsymbol{E} = E_0 \cos(\boldsymbol{k}\cdot\boldsymbol{x} - \omega t) \boldsymbol{v}_p$$

where  $\boldsymbol{v}_p$  represents the polarization of the wave.

### B.1 Light intensity

In classical electrodynamics, it is possible to define a vector which describes the flow of energy in the electromagnetic field. The expression of this vector, called Poynting vector, in a vacuum is:

$$\boldsymbol{\pi} = \epsilon_0 c^2 \boldsymbol{E} \wedge \boldsymbol{B}$$

with  $\epsilon_0 \approx 8.85 \times 10^{-12} \text{ F m}^{-1}$  the vacuum permittivity and the magnetic field  $\boldsymbol{B}$  for a plane wave is given by:

$$\boldsymbol{B} = \frac{1}{c\|\boldsymbol{k}\|} \boldsymbol{k} \wedge \boldsymbol{E}$$

Averaging the norm of the Poynting vector over one temporal period, we get the electromagnetic intensity of the field:

$$I_{EM} = \frac{1}{2} c \epsilon_0 E_0^2$$

This physical quantity is to be compared with

$$I_{sat} = \frac{\hbar^2 c \epsilon_0 \Gamma^2}{2d^2}$$

where  $\Gamma$  is the natural linewidth of the atomic transition and  $d = \langle 2 | \hat{\mathbf{D}} \cdot \mathbf{v}_p | 1 \rangle$ <sup>1</sup>.  $\hat{\mathbf{D}}$  is the dipole operator of quantum mechanics.

We can introduce the laser saturation parameter

$$s_0 = \frac{I_{EM}}{I_{sat}}$$

## B.2 Atomic saturation parameter

The relevant parameter that measures the saturation of the targeted atomic transition is the atomic saturation parameter:

$$s = s_0 \frac{1}{1 + \left( \frac{\delta\omega_{tot}}{\Gamma} \right)^2}$$

It takes into account the laser's detuning with respect to the resonance of the atomic transition, as well as the Doppler effect:

$$\delta\omega_{tot} = \delta\omega_{laser} + \delta\omega_{Doppler} = \omega - \omega_0 - \mathbf{k} \cdot \mathbf{v}$$

The Doppler detuning term describes the fact that if the atom goes towards the laser, it will see laser light that has a higher frequency than what the laser operator would measure in the reference frame of the laboratory.

## B.3 Radiation pressure

Using a semi-classical model (optical Bloch equations for the internal state of the atom and a classical electromagnetic field), we can compute the radiation pressure exerted on the atom [13]:

$$\mathbf{F}_{rad} = \frac{\Gamma}{2} \frac{s}{1+s} \hbar \mathbf{k}$$

This formula has a rather satisfying physical interpretation:  $\frac{\Gamma}{2} \frac{s}{1+s}$  is in fact the number of fluorescence cycles (absorption-spontaneous emission) the atom undergoes and  $\hbar \mathbf{k}$  is the momentum carried by a photon. This formula describes the conservation of momentum when a photon is absorbed by the atom, which is afterwards emitted spontaneously in a random direction. The direction of the incident photons is fixed and therefore on average, the atom only feels the pushing force exerted by the incident photons.

---

<sup>1</sup>We chose the phase of  $|1\rangle$  and  $|2\rangle$  to have  $d \in \mathbb{R}$ .

## **B.4 Dipole force**

When the amplitude of the electric field is not constant (contrary to the plane wave we described), there is an additional force exerted on the atom called dipole force. Regions of high electromagnetic energy density can repel or attract atoms depending on the laser detuning, and this phenomenon is explained with the dipole force.

## Appendix C

# Piecewise quadratic interpolation of the electric potential

To compute the total energy of the system, we need to know the value of the electric potential on the ion's trajectory. The real electric field is however only known only on a finite and periodic lattice in 3D space, meaning the code has to guess the value of the field between the nodes of the lattice. It does so by linear interpolation of the electric field.

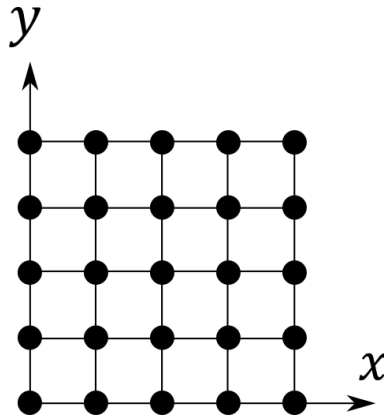


**Figure C.1:** 2D periodic lattice. Black points represents the nodes.

The ions in the simulation feel an electric field that is piecewise linear. It means, that on each cell defined by the lattice, the electric field is of the form:

$$E_x = \lambda_1 x + \lambda_2 y + \lambda_3 z + \lambda_4$$

$$E_y = \lambda_5 x + \lambda_6 y + \lambda_7 z + \lambda_8$$

$$E_z = \lambda_9 x + \lambda_{10} y + \lambda_{11} z + \lambda_{12}$$

The coefficients  $\lambda_i$  are different from one cell to another, but they are not independent because the

electric field is continuous. Also, the real electric field obeys Maxwell's equations. We suppose the linear approximation does as well, although it is strictly speaking not the case, which introduces dependencies between the  $\lambda_i$  belonging to the same cell.

Consequently, there is an electric potential from which the electric field can be derived of the form:

$$\Phi = \mu_1 x^2 + \mu_2 y^2 + \mu_3 z^2 + \mu_4 xy + \mu_5 xz + \mu_6 yz + \mu_7 x + \mu_8 y + \mu_9 z + \mu_{10}$$

The coefficients  $\mu_i$  are different from one cell to another.  $-\nabla\Phi = \mathbf{E}$  yields simpler relations for the electric field:

$$\begin{aligned} -E_x &= 2\mu_1 x + \mu_4 y + \mu_5 z + \mu_7 \\ -E_y &= \mu_4 x + 2\mu_2 y + \mu_6 z + \mu_8 \\ -E_z &= \mu_5 x + \mu_6 y + 2\mu_3 z + \mu_9 \end{aligned}$$

The potential coefficients  $\mu_1 \dots \mu_9$  are easy to compute for each cell if we evaluate the linear interpolation of the electric field on wisely chosen points. Doing this operation on the cubic potential trap, we get the following piecewise quadratic interpolation of the potential.

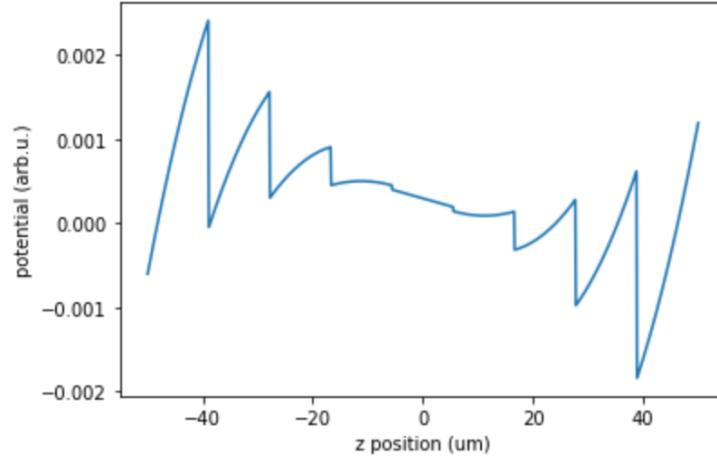


**Figure C.2:** Piecewise quadratic interpolation of the cubic potential trap

We need to adjust the last potential coefficient  $\mu_{10}$  for each cell in order to construct a continuous potential. Doing so, we get:

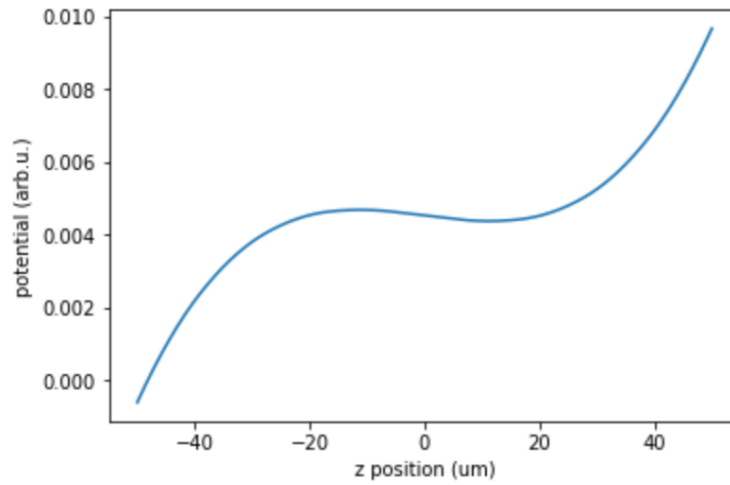


**Figure C.3:** *Continuous piecewise quadratic interpolation of the cubic potential trap*

We recognize the wanted shape of the potential. For fields that are simple enough, the proposed method is able to construct a continuous piecewise quadratic potential, but for more complex fields, the method fails to do so, although the remaining discontinuities are in general small.

# Bibliography

- [1] P. Schmidt et al. “Spectroscopy Using Quantum Logic”. In: *Science* 309 (2005), pp. 749–752.
- [2] D. Kielpinski et al. “Architecture for a large-scale ion-trap quantum computer”. In: *Nature* 417 (2002), pp. 709–711.
- [3] S. Seidelin et al. “Microfabricated Surface-Electrode Ion Trap for Scalable Quantum Information Processing”. In: *Physical review letters* 96 (July 2006), p. 253003.
- [4] M. Niemann et al. “Cryogenic  $^9\text{Be}^+$  Penning trap for precision measurements with (anti-)protons”. In: *Measurement Science and Technology* 31 (Dec. 2019), p. 035003.
- [5] D. Griffiths. *Introduction to Electrodynamics*. Ed. by Pearson. 2013.
- [6] J. D. Jackson. *Classical Electrodynamics*. Ed. by John Wiley and Inc. Sons. 1999.
- [7] D. Leibfried et al. “Quantum dynamics of single trapped ions”. In: *Reviews of Modern Physics* 75 (Jan. 2003).
- [8] D. Kienzler. “Quantum Harmonic Oscillator State Synthesis by Reservoir Engineering”. PhD. ETH Zurich, 2015.
- [9] K. R. Brown et al. “Coupled quantized mechanical oscillators”. In: *Nature* 471 (Mar. 2011), pp. 196–199.
- [10] A. C. Wilson et al. “Tunable spin–spin interactions and entanglement of ions in separate potential wells”. In: *Nature* 512 (Aug. 2014), pp. 57–60.
- [11] M. Guggemos et al. “Sympathetic cooling and detection of a hot trapped ion by a cold one”. In: *New Journal of Physics* 17 (Sept. 2015), p. 103001.
- [12] D. Kielpinski et al. “Two-mode coupling in a single-ion oscillator via parametric resonance”. In: *American Physical Society* 89 (June 2014), p. 062332.
- [13] G. Grynberg, A. Aspect, and C. Fabre. *Introduction to quantum optics*. Ed. by Cambridge University Press. 2010.